Characteristics of 3D printing resin in accordance with different surface treatment times of zirconia filler with 10-MDP

Gi-Tae Kim

The Graduate School
Yonsei University
Department of Applied Life Science

Characteristics of 3D printing resin in accordance with different surface treatment times of zirconia filler with 10-MDP

A Dissertation Thesis

Submitted to the Department of Applied Life Science

and the Graduate School of Yonsei University

in partial fulfillment of the

requirements for the degree of

Ph.D. in Applied Life Science

Gi-Tae Kim

June 2024

This certifies that the Doctoral Dissertation

of 'Gi-Tae Kim' is approved.

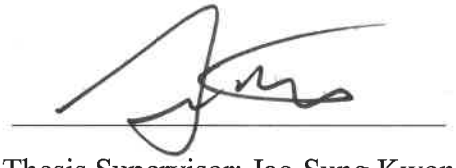

Thesis Supervisor: Jae-Sung Kwon

Kwang-Mahn Kim: Thesis Committee Member #1

Sung-Hwan Choi: Thesis Committee Member #2

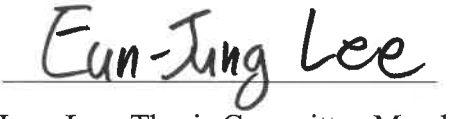

Eun-Jung Lee: Thesis Committee Member #3

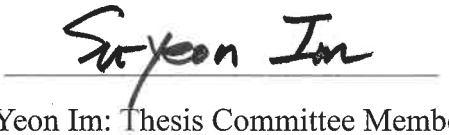

Su-Yeon Im: Thesis Committee Member #4

The Graduate School

Yonsei University

June 2024

ACKNOWLEDGEMENTS

In the summer of 2021, I completed my master's degree and embarked on a new challenge: pursuing a doctoral degree. Although I was apprehensive about the long and arduous journey ahead, I was excited about the changes and growth it would bring to my life. Now, in the summer of 2024, I am graduating from the doctoral program. I would like to express my gratitude to those who have supported and guided me, despite my shortcomings.

First and foremost, I would like to express my sincere gratitude to *Prof. Kwang-Mahn Kim*, who has laid the foundation for my research and guided me in the right direction throughout my master's and doctoral degrees. I would also like to express my deepest gratitude to my advisor, *Prof. Jae-Sung Kwon*, who leads the Department of Dental Biomaterials and Bioengineering. Whenever I encountered difficulties during my research, he provided me with wise counsel, insightful advice, and generous guidance, helping me navigate through the challenges. I am grateful to *Prof. Sung-Hwan Choi*, who has inspired me with his passion and drive for research and has always encouraged me when faced with challenges. I am thankful to *Prof. Eun-Jung Lee*, who has patiently answered even my most trivial questions, meticulously reviewed my research, and provided heartfelt advice. I express my profound gratitude to *Prof. Su-Yeon Im*, who has offered meticulous guidance, warm consideration, and unstinting advice, helping me find my way forward even in difficult situations and providing me with various opportunities.

I also sincerely thank the members of the Department and Research Institute of Dental Biomaterials and Bioengineering. I have made many memories and gained valuable experience through my interactions with these wonderful teachers. Without their help, I would not have been able to complete my research successfully.

I dedicate this honor to my beloved father, mother, and younger sibling. Their unconditional love and unwavering support have made me who I am today. Words cannot express the

depth of my gratitude for their presence in my life, and I will always cherish them. I bow my head in gratitude once again to my family, who have been my silent pillars of strength throughout the long journey of my master's and doctoral studies. I love you all.

Finally, I thank God for the lessons He has taught me throughout this entire process. It is through His guidance that I have been able to overcome all adversities and embrace today's glory.

Once again, I sincerely thank everyone who has guided and supported me.

TABLE OF CONTENTS

LIST OF FIGURES

LIST OF TABLES

ABSTRACT

Characteristics of 3D printing resin in accordance with different surface treatment times of zirconia filler with 10-MDP

Gi-Tae Kim

Department of Applied Life Science

The Graduate School, Yonsei University

(Directed by Professor Jae-Sung Kwon, M.D., Ph.D.)

Three-dimensional printing systems are widely utilized in dentistry due to their ability to streamline manufacturing processes, reduce production times, and enable personalized fabrication. For the fabrication of fixed dental prostheses, the mechanical properties, physical properties, conversion rate, accuracy, and biocompatibility of 3D printing resin are crucial. Particularly, due to the necessity of withstanding occlusal forces, research to enhance mechanical properties for clinical application was required. Zirconia fillers in 3D printing resins offer various advantages such as superior mechanical properties, biocompatibility, and excellent wear resistance. However, zirconia fillers lack chemical affinity with silane coupling agents. To overcome these limitations, 10-Methacryloyloxydecyl dihydrogen phosphate (10-MDP) was used as a surface modifier for the zirconia fillers. The 10-MDP molecule has a phosphate group at one end, which can

form chemical bonds with zirconia, and a methyl methacrylate group at the other end, which can polymerize with the resin matrix. Therefore, surface treatment of zirconia fillers with 10-MDP is expected to modify the zirconia surface. The purpose of this study was to produce optimized surface-modified zirconia fillers using various exposure times for surface treatment with 10-MDP, and to incorporate the surface-treated fillers into 3D printing resin to improve mechanical properties.

Zirconia filler was surface treated using 10-MDP solution. The control group was commercial 3D printing resin, while the experimental groups consisted of the 0D group with untreated zirconia filler added, and the 1D, 7D, and 14D groups containing zirconia fillers surface-treated for 1 day, 7 days, and 14 days, respectively. To confirm the surface treatment of the fillers, transmission electron microscopy (TEM), thermogravimetric analyzer (TGA), and X-ray photoelectron spectroscope (XPS) analyses were conducted. Surface-treated zirconia fillers at 5 wt.% were mixed with commercial 3D printing resin. The specimens were designed using a CAD program and printed with a DLP 3D printer. Post-processing was conducted on the 3D-printed specimens. The experiments measured mechanical properties, water sorption and solubility, degree of conversion, dimensional accuracy, and cytotoxicity.

All surface-treated zirconia fillers were observed to have organic compounds attached in the TEM images. TGA results showed weight loss in the temperature range of 100 °C to 450 °C. In the XPS results, Zr-O-P bonds were observed. According to the TEM, TGA, and XPS results, 10-MDP was demonstrated to successfully treat the surface of the zirconia fillers. The flexural strength and modulus in the 0D group was consistently the lowest regardless of the storage conditions, with the 7D and 14D groups showing significantly higher values than the other groups ($p < 0.05$). In terms of microhardness, the control group showed significantly lower values, while the 14D group showed significantly higher results ($p < 0.05$). In the water sorption test, the 7D and 14D groups showed significantly lower values compared to the control group. However, in the water solubility test, the 1D, 7D, and 14D groups exhibited significantly higher values compared to the control group ($p <$

0.05). In terms of dimensional accuracy, the results for the XY-axis showed that all groups except the control group were closer to the true value ($p < 0.05$). The degree of conversion and cytotoxicity did not show significant differences in all groups ($p > 0.05$).

In conclusion, it was demonstrated that surface treatment of zirconia filler using 10-MDP is feasible. Additionally, the addition of surface-treated zirconia was shown to influence the properties of 3D printing resin. Moreover, the optimal surface treatment exposure time was determined to be 7 days. The surface-treated zirconia fillers with 10-MDP incorporated into 3D printing resin exhibited no cytotoxicity and demonstrated the potential to enhance mechanical properties without adversely affecting dimensional accuracy. Therefore, surface-treated zirconia fillers with 10-MDP can be sufficiently utilized as fillers for dental 3D printing resins.

Key words: Surface treatment, 10-MDP, zirconia filler, 3D printing resin, chemical bonding

Characteristics of 3D printing resin in accordance with different surface treatment times of zirconia filler with 10-MDP

Gi-Tae Kim

Department of Applied Life Science

The Graduate School, Yonsei University

(Directed by Professor Jae-Sung Kwon, M.D., Ph.D.)

I. INTRODUCTION

1. Zirconia filler

Zirconium dioxide (ZrO_2), commonly known as zirconia, possesses many attractive properties such as ion-exchange capability, high refractive index, low thermal conductivity, low coefficient of thermal expansion, and a polymorphic nature (Bannunah, 2023; Gurushantha et al., 2015). Zirconium dioxide is a commercially economical, non-hazardous, and sustainable metal oxide with diverse potential applications (Keiteb et al., 2016). Zirconia is widely used in the medical engineering industry as an advanced biomaterial due to its excellent biocompatibility and mechanical strength (Bannunah, 2023).

Zirconia has been introduced to dentistry due to its superior mechanical properties (strength, toughness, fatigue resistance, low elastic modulus, and fracture strength),

biocompatibility, and excellent wear resistance (Palmero et al., 2015; Seo et al., 2020; Wille et al., 2016). Furthermore, the addition of 5 wt.% zirconia to dental resin improved the antibacterial capability of the resin without inducing cytotoxicity (Aati et al., 2022). Studies have shown that the addition of modified zirconia particles (≤ 5 wt.%) enhances mechanical, physical, and/or biological properties, including flexural strength, fracture toughness, hardness, wear resistance, thermal stability, and biocompatibility of the composites (Ergun et al., 2018; Gad et al., 2019; Maji et al., 2016).

2. Inorganic fillers and surface treatment

The basic composition of dental resin primarily consists of a resin matrix and inorganic filler (Ferracane, 2011). The inorganic filler majorly contributes to the mechanical properties of the resin. According to research, the content, type, shape, and particle size of the inorganic filler have been confirmed to significantly impact the mechanical and physical properties of dental resin. These effects are mainly manifested in wear resistance, flexural strength, elastic modulus, polymerization shrinkage, water sorption and solubility, as well as antimicrobial properties (Randolph et al., 2016; Shah and Stansbury, 2014).

Inorganic fillers cannot form a direct chemical bond with the resin matrix until they are surface-treated with a coupling agent to mediate the bonding (Cramer et al., 2011; Habib et al., 2016). Therefore, enhancing the bonding between inorganic fillers and the resin matrix is particularly important. In silica-based fillers, which are often used as inorganic fillers, silane molecules are generally hydrolyzed to become silanol groups, which form hydrogen bonds with hydroxyl groups on the filler surface and are silanized by dehydration condensation (Aydınoğlu and Yoruç, 2017).

However, zirconia fillers have chemically inert and non-polar surfaces, thus silane coupling agents lack chemical affinity to the zirconia surface (Alhavaz et al., 2017). The mechanical properties of dental resins can be further enhanced if suitable surface treatments can be adopted in order to activate the zirconia filler surface to chemically bond with the resin matrix (Wu et al., 2019).

3. 10-methacryloyloxydecyl dihydrogen phosphate

Phosphate ester monomers have been shown to chemically bond with zirconia. Among the various phosphate ester monomers available, the bonding improvement of 10-methacryloyloxydecyl dihydrogen phosphate (10-MDP) has been demonstrated (Inokoshi et al., 2014; Thompson et al., 2011; Tzanakakis et al., 2016). According to the references of Gomes et al. and Yoshida et al., primers and cements containing 10-MDP have shown high bond strength and durability with zirconia (Gomes et al., 2013; Yoshida et al., 2006).

The 10-MDP molecule has a phosphoric-acid group on one end, which acts as an adhesion promoter for metal oxides, including zirconia. On the other end of the molecule, there is a methyl methacrylate group that enables polymerization with the unsaturated carbon bonds present in the resin matrix. These two active groups are separated by a spacer ester chain composed of ten carbons (Chen et al., 2017a). Several studies have confirmed the possibility of chemical bonding between zirconia and 10-MDP through experiments such as Time-of-flight secondary ion mass spectrometry, Fourier transform infrared spectroscopy, X-ray photoelectron spectroscopy, and Nuclear magnetic resonance spectroscopy (Nagaoka et al., 2017; Pilo et al., 2016; Wu et al., 2019; Xie et al., 2016; Ye et al., 2022).

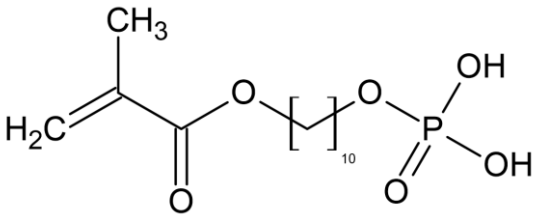

Figure 1. Chemical structures of 10-methacryloyloxydecyl dihydrogen phosphate.

4. Reaction mechanism between 10-MDP and zirconia

Pure 10-MDP exists in a sticky colloidal form. Therefore, solvents such as ethanol or acetone are needed for dispersion. According to research, the most effective concentration range of 10-MDP for optimal interaction between 10-MDP and hydroxyapatite is 5 to 10 % (Tian et al., 2016). Various treatment times have been applied to modify the surface of zirconia, but there has been no optimized research on the surface treatment time of zirconia fillers (Chen et al., 2017b; Wu et al., 2019; Yang et al., 2020).

10-MDP can form stable Zr-O-P bonds with zirconia atoms on the surface of zirconia after dissociation in a solvent, and the unsaturated C=C bond on the other end of 10-MDP can polymerize with the methacrylate in the resin matrix (Chen et al., 2017b; Xie et al., 2015). Recent studies have shown that resin composites using bisphenol-glycidyl dimethacrylate (Bis-GMA) and urethane dimethacrylate (UDMA) resins with 10-MDP conditioned zirconia fillers exhibit superior flexural strength, elastic modulus, and surface hardness in *in vitro* tests compared to resin composites using unmodified zirconia fillers (Wu et al., 2019; Yang et al., 2020). This suggests that surface treatment of zirconia fillers with 10-MDP can potentially generate micro-zirconia fillers suitable for application in dental resins.

The chemical reaction mechanism between zirconia and 10-MDP is shown in Figure 2, with reference to the papers (Chen et al., 2017a; Xie et al., 2015).

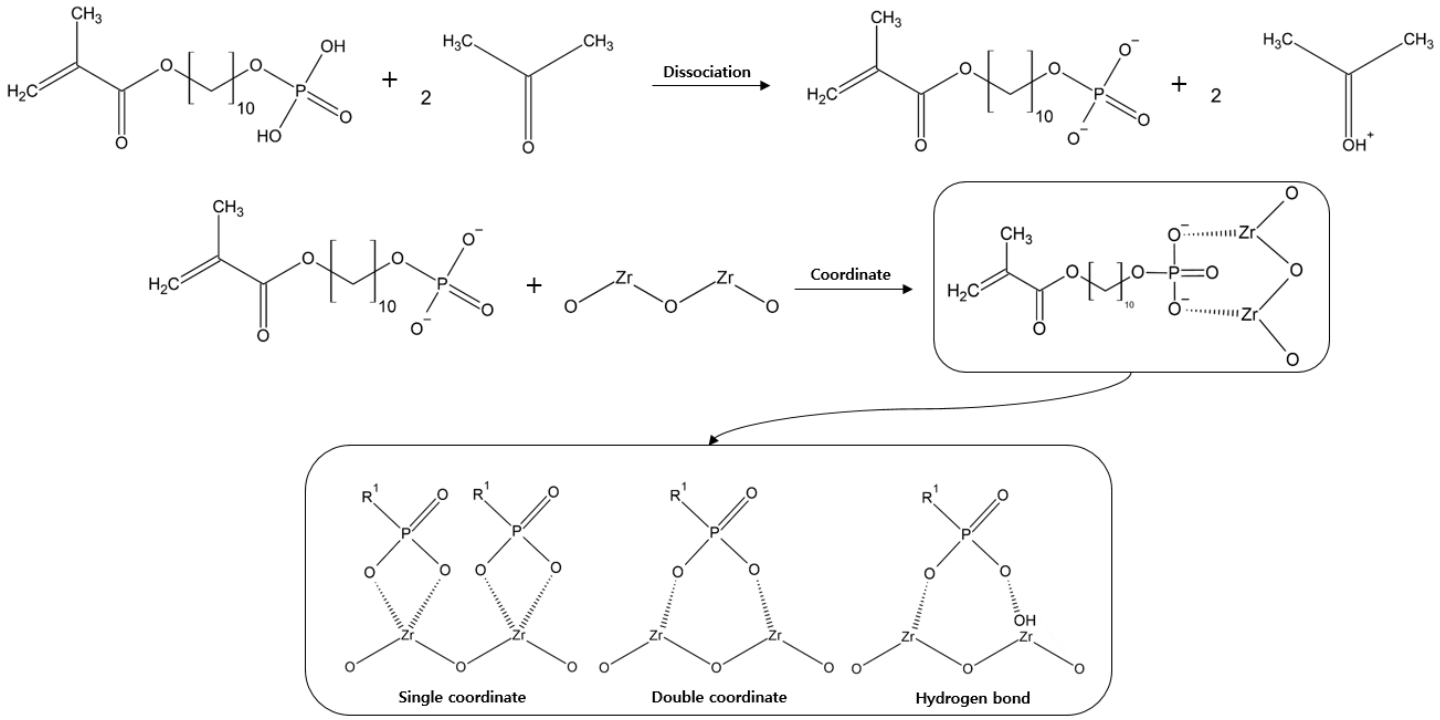

Figure 2. Reaction pathways of 10-MDP coordinated with zirconia in the acetone solvents.

5. Dental 3D printing technologies

5.1. 3D printing system

The Computer-Aided Design/Computer-Aided Manufacturing (CAD/CAM) system has been a major impact on the dental field by simplifying the process and reducing production time (Abduo et al., 2014; Van Noort, 2012). 3D printing system that corresponds to additive manufacturing has the advantage of being able to create complex shapes, personalized production and consuming less material (Della Bona et al., 2021; Moon et al., 2021). The most commonly used 3D printing methods in dentistry include stereolithography apparatus (SLA) and Digital Light Processing (DLP), which use light-cured resin, Fused Deposition Modeling (FDM) that utilizes thermoplastic material, and Selective Laser Sintering (SLS) that employs laser-sinterable powder (Dawood et al., 2015; Punia et al., 2022).

Among the 3D printing methods, Digital Light Processin (DLP) is the method of irradiating light in tanks containing light-cured resin which reacts with ultraviolet and producing prosthetics through photo-polymerization (Moon et al., 2021). DLP technology contains a microsystem with a rectangular mirror arrangement called a digital micromirror device. The angle of the micromirrors can be individually adjusted. The micromirrors, which act as light switches, project the light from the source onto the projection surface. The advantage of DLP technology is that every layer can be cured with a single shot of laser exposure by producing laser light. This advantage makes the printing time independent of the layer geometry or the number of objects (Kessler et al., 2020; Punia et al., 2022).

5.2. 3D printing resin

The ingredients of a light-cured resin include a matrix, a filler and a photoinitiator to ensure the properties of the material (Albuquerque et al., 2013). The resin matrix consists of dimethacrylate monomers such as urethane dimethacrylate, bisphenol-A-ethoxy dimethacrylate, or triethyleneglycol dimethacrylate (Wang et al., 2021). A photoinitiator system is added to the resin matrix to trigger the free radical process in the polymerization reaction (Kim et al., 2022). Curing occurs after photoinitiators generate free radicals under the suitable UV-light source, and monomers start to form bonds through the chain radical polymerization mechanism (Ribas-Massonis et al., 2022).

Dental 3D printing resins can be used to make prostheses such as surgical guides, crowns & bridges, and dentures (Stansbury and Idacavage, 2016). The cytotoxicity and accuracy are very important as the dental 3D printed resin is placed in the patient's oral cavity (Aati et al., 2021). Furthermore, 3D printed resins when applied for temporary fixed dental prostheses must withstand occlusal forces, making it essential to ensure sufficient mechanical properties for clinical application (Reymus et al., 2020). The inclusion of fillers in printable resins can increase the viscosity, leading to poor printability and issues such as uneven flow, and decreased accuracy (de Castro et al., 2016; Mubarak et al., 2020). Therefore, recent studies have emphasized the development of printable resins with modified fillers added to optimize the mechanical properties of temporary prostheses made by 3D printing (Aati et al., 2021).

6. Research objectives

Zirconia fillers offer various advantages in dentistry, such as excellent mechanical properties, biocompatibility, and superior wear resistance. However, a challenge with zirconia fillers is their difficulty in surface treatment. Furthermore, while there are numerous studies on adding zirconia fillers to dental composite resins, research on adding them to dental 3D printing resins and examining their properties is scarce.

The purpose of this study was to produce optimized surface-modified zirconia fillers using various exposure times for surface treatment with 10-MDP, and to incorporate the surface-treated fillers into 3D printing resin to improve mechanical properties.

The null hypothesis is that there would be no differences in the mechanical properties, water absorption and solubility, degree of conversion, dimensional accuracy, and cytotoxicity among 3D printing resins with zirconia fillers modified with various surface treatment times using 10-MDP.

II. MATERIALS AND METHODS

1. Surface treatment of zirconia fillers with 10-MDP

In this study, Zirconium (IV) oxide (ZrO_2; Sigma-Aldrich, Steinheim, Germany) was used as the filler. Zirconium oxide powders were heated to 550 °C for 30 min to remove organic contaminants. The 10-MDP solution was a mixture of 90 wt.% of acetone (Acetone; Duksan reagents, Ansan, Korea) and 10 wt.% of 10-methacryloyloxydecyl dihydrogen phosphate (10-MDP; SY Innovation, Pyeongtaek, Korea). Zirconia powders were immersed in the 10-MDP solution at a concentration of 1 g/ml. The mixture of zirconia powder and 10-MDP solution was probe-sonicated using a probe type high energy sonicator (Q125 Sonicator, Qsonia LLC, Newtown, CT, USA) for 20 min. The sonication cycle consisted of 10 s of operation at 40 % amplitude, followed by 15 s resting intervals. After sonication, the mixture was divided into three groups, which were immersed at room temperature for 1 day, 7 days, and 14 days, respectively. After the immersion period, the mixture was centrifuged at 3088 × g for 3 min using a centrifuge. To collect the surface-treated zirconia filler, the separated solution was removed from the filler.

2. Characterization of zirconia surface treated with 10-MDP

2.1. Morphology

The morphology of zirconia filler and surface-treated zirconia filler was examined by transmission electron microscopy (TEM; JEM-200F, JEOL, Tokyo, Japan). Each 0.1 mg sample was dispersed in 1 mL of acetone. A drop of suspension was then settled on a TEM grid (200 mesh) and dried.

2.2. Measurement of 10-MDP surface teatment quantity on zirconia fillers

The surface-treatedzirconia filler was analyzed using a thermogravimetric analyzer (TGA; Q50, TA Instruments, New Castle, USA) to determine the amount of 10-MDP bonded to the surface of the zirconia filler. Neat zirconia filler was used as the control. Approximately 20 mg of each surface-treated zirconia filler was placed in an alumina crucible and heated in a nitrogen atmosphere from 40 to 450 °C at a rate of 10 °C/min.

2.3. Chemical property

The chemical bond between 10-MDP and zirconia was confirmed using an X-ray photoelectron spectroscope (XPS; K-alpha, Thermo Fisher Scientific, Waltham, USA) with monochromated Al Kα radiation. The O1s spectra were processed using XPS Peak 4.1 software. The relative content of chemical bonds (Zr-O-P, Zr-O-Zr, P-OH / C-O) was determined based on the peak area.

3. Preparation of 3D printing C&B resin incorporating zirconia filler

The surface-treated zirconia filler was homogeneously dispersed in the 3D printing C&B resin (Nextdent C&B; NextDent, Soesterberg, Netherlands) by a solvent-based mixing method using acetone. Composition of 3D printing C&B resin is listed in Table 1.

The schematic diagram of the preparation process of 3D printing C&B resin incorporating surface-treated zirconia fillers is shown in Figure 3. The surface-treated zirconia filler was mixed with acetone in a weight ratio of 5 : 1 (surface-treated zirconia filler : acetone). The surface-treated zirconia suspension was then added to the 3D printing C&B resin at a concentration of 5 wt.%, and the mixture was homogenized using a speed mixer (DAC 105.1 FVZ, Hauschild SpeedMixer, Hamm, Germany) at 3500 rpm for 3 min. After that, the acetone in the mixture of the zirconia filler suspension and 3D printing C&B resin was slowly evaporated in a dark environment by magnetic stirring at 1000 rpm, 60 °C for 12 h. Air bubbles were removed under a vacuum at 10 min. The completed 3D printing C&B resin incorporating surface-treated zirconia filler was used. Prior to printing, the 3D printing C&B resin with surface-treated zirconia fillers was mixed again using a speed mixer at 3500 rpm for 3 min to ensure homogeneity.

The group codes were set as shown in Table 2. The control group used 3D printing C&B resin. For the experimental groups, the group with 3D printing resin containing untreated zirconia filler was designated as the 0D group. The 3D printing resin groups containing surface-treated zirconia filler were classified according to the surface treatment time. The group with 1 day of surface treatment was classified as the 1D group, the group with 7 days of surface treatment as the 7D group, and the group with 14 days of surface treatment as the 14D group.

Table 1. Composition of 3D printing C&B resin

Composition	Wt.%
Ethoxylated bisphenol A dimethacrylate	≥ 75 %
7,7,9(or 7,9,9)-trimethyl-4,13-dioxo-3,14-dioxa-5,12-diazahexadecane-1,16-diyl bismethacrylate	10 - 20
Phenyl bis(2,4,6-trimethylbenzoyl)-phosphine oxide	< 10 %
Titanium dioxide	0.1 - 1

www.nextdent.com

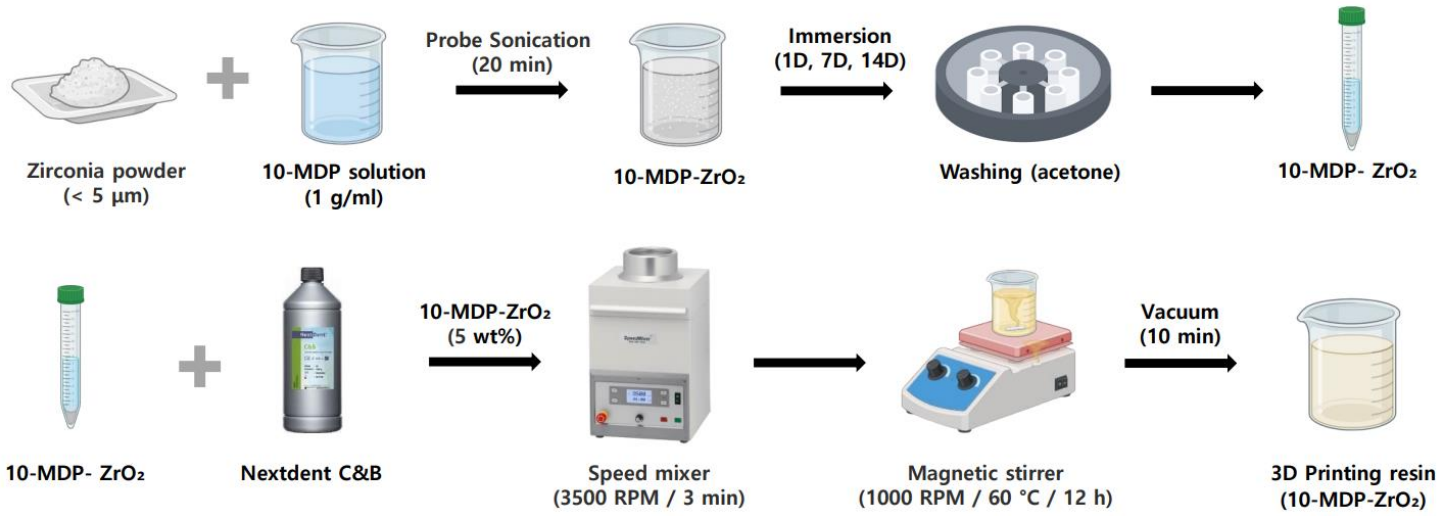

Figure 3. Description of the preparation process of 3D printing C&B resin incorporating surface-treated zirconia fillers.

Table 2. Exposure time for 10- MDP surface treatment of zirconia filler and experimental codes

Group code	3D printing C&B resin (wt. %)	Zirconia filler (wt. %)	Surface-treatment time (Days)
CTL	100	0	0
0D	95	5	0
1D	95	5	1
7D	95	5	7
14D	95	5	14

.

4. Preparation of 3D printed specimens

3D printer software (3D Sprint; 3D systems, Soesterberg, Netherlands) was used for designing the specimen. The Specimens required for each test were designed. After adding supporters to the specimen design, it was converted to a standard tessellation language (STL) format.

All specimens were manufactured using a DLP printer (Nextdent 5100; 3D Systems, Soesterberg, Netherlands). The wavelength was 405 nm, and the layer thickness was set to 50 μm. The 3D-printed green phase specimen was placed in a beaker containing isopropyl alcohol (IPA; LG Chem Ltd., Yeosu, Korea), and ultrasonically cleaned for 3 min. After that, support structures were removed using the finish kit (Form 2 Finish Kit; Formlabs Inc., Somerville, MA, USA), and ultrasonic cleaning was performed for 2 min in the same method. After removing all remaining IPA with an air gun, specimens were put into a post-curing unit (LC-3D Print Box; 3D systems, Soesterberg, The Netherlands) with a wavelength band of 350 to 500 nm and cured for 10 min.

5. Mechanical properties

5.1. Flexural strength and modulus

5.1.1. Design and printing for flexural strength and modulus

The specimens (n=10) for flexural strength and modulus were referenced to the ISO 4049:2019 standard (ISO, 2019). The specimens were designed as shown in Figure 4. The specimens for three-point flexural strength were printed with dimensions of 25 × 2 × 2 mm.

Specimen preparation was performed in the same method as in section 4. The residual support structures of 3D printed specimen were polished using a water-cooled rotating polishing machine (Ecomet 30; Buehler Ltd., Lake Bluff, IL, USA) with #320 grit silicon carbide paper.

All specimens were prepared and divided into two groups. Half of the specimens were immersed in water at 37 ℃ for 24 h, while the remaining specimens were stored at room temperature for the same time.

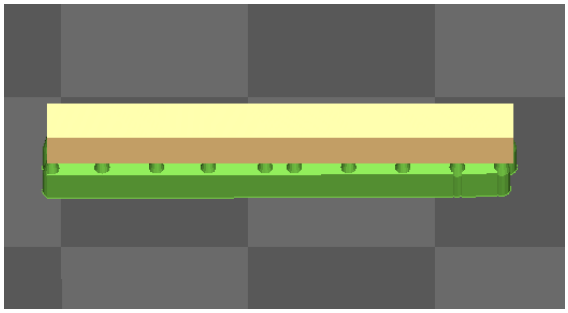

Figure 4. STL image of the specimen for three-point bending test, displaying the designed specimen (yellow) and the support structure (green) for 3D printing.

5.1.2. Flexural strength and modulus analysis

Flexural strength and modulus were carried out on a universal testing machine (Instron 5942; Instron, Norwood, MA, USA). The crosshead speed was 1 mm/min and the distance between the two rounded supports was 20 mm. The load was applied until the specimen was fractured. The maximum load was recorded, and the flexural strength (*S*) and modulus (*E*) were calculated using the following equation:

$$S = \frac{3Fl}{2bh^2}$$

$$E = \frac{F_1 l^3}{4bh^3 d}$$

Where *F* is the maximum fracture load, l is the distance of support (20 mm), *b* is the width of specimen, and *h* is height of specimen (mm). F_1 is the load at a point in the straight-line portion of the load/displacement curve (N), and d is the deflection at load F_1 (mm).

5.1.3. Fractured surface analysis

To observe the morphology and pattern of the fractured surface, surface images of fractured specimens were acquired using a scanning electron microscope (JSM-7800F; JEOL Ltd., Akishima, Japan) with an accelerating voltage of 30 kV. The fractured surface specimens were coated with a 5 nm thick layer of gold using an ion coating machine (ACE600; Leica, Wetzlar, Germany) SEM images were captured at 5000 × magnification.

The distribution of zirconia filler or surface-treated zirconia fillers in the fracture section was explored through zirconium and phosphorus element mapping under the same SEM observation settings.

5.2. Microhardness

5.2.1. Design and printing for microhardness

The specimen (n=10) for microhardness test was disc-shaped, 10 mm in diameter and 5 mm in height. Specimen preparation was performed in the same method as in section 4. The prepared disk specimens were polished with #400, #800 and #1200 grit silicon carbide paper a using water-cooled rotating polishing machine (Ecomet 30; Buehler Ltd., Lake Bluff, IL, USA).

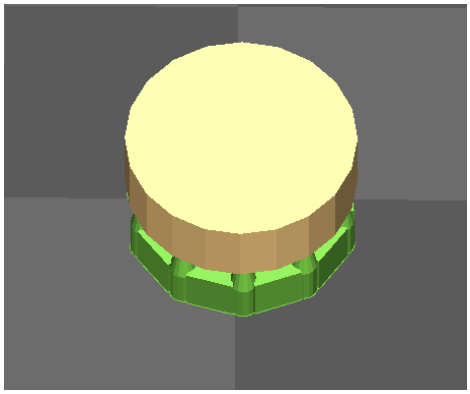

Figure 5. STL image of the specimen for microhardness measurement, displaying the designed specimen (yellow) and the support structure (green) for 3D printing.

5.2.2. Microhardness test

The samples were placed in a Vickers hardness tester (MMT-X; Matsuzawa Ltd., Akita, Japan), and 0.98 N (100 gf) was applied for 10 s. The indentation was observed, and the Vickers hardness number (VHN) was measured to determine the surface hardness. Three sites were measured at random for each specimen, and the mean value and standard deviation were obtained. The hardness was determined using the following equation:

$$\mathrm{VHN} = 1.854\frac{F}{d^2}$$

Where *F* is the indentation load and *d* is the arithmetic mean of two diagonals (mm).

6. Water sorption and solubility

6.1. Design and printing for water sorption and solubility

The water absorption and solubility of the experimental 3D printing resin were performed according to ISO 4049:2019 (ISO, 2019). The specimens were designed as shown in Figure 6. The specimen (n=10) of water sorption and solubility was disc-shaped, 15 mm in diameter and 1.0 mm in height. Specimen preparation was performed in the same method as in section 4. The residual supporters of 3D printed specimen were polished to #1000 grit silicon carbide paper.

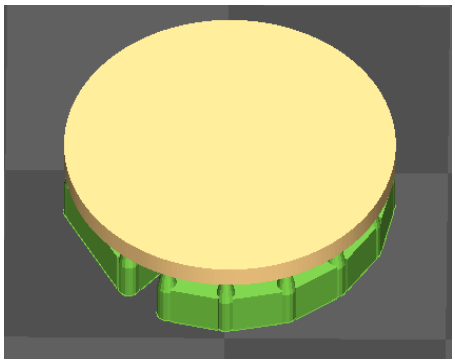

Figure 6. STL image of the specimen for water sorption and solubility measurement, displaying the designed specimen (yellow) and the support structure (green) for 3D printing.

6.2. Water sorption and solubility test

The specimen was placed in a desiccator maintained at (37 ± 2) ˚C. After 22 h, the specimen was removed and kept in a desiccator at (23 ± 1) ˚C for 2 h. An analytical balance (ME204T; Mettler-toledo AG, Greifensee, Switzerland) with an accuracy of 0.01 mg and a reproducibility of 0.1 mg was used to measure the weight of the specimen until a constant mass (m_1) was reached.

The size of the specimen was measured using a digital caliper (Mitutoyo Model CD-15CPX; Mitutoyo Corporation, Kawasaki, Japan) with an accuracy of 0.01 mm. The average diameter was calculated by measuring three diameters. The average thickness value was calculated by measuring three equally spaced points on the circumference. The measured values were used to calculate the volume (V) of all specimens (in 0.01 mm^3).

After that, the specimens were stored in distilled water at (37 ± 1) ˚C for 7 d, blotted to remove visible moisture, waved in the air for 15 s, and weighed for mass (m_2).

Finally, each specimen was placed in a desiccator and weighed daily until a constant dry mass (m_3) was obtained. Water sorption and solubility were calculated using the following equations:

$$W_{sp} = \frac{(m_2 - m_3)}{V}$$

$$W_{sl} = \frac{(m_1 - m_3)}{V}$$

Where W_{sp} is the absorption of the test material (μg/mm^3), W_{sl} is the solubility of the test material (μg/mm^3).

7. Degree of conversion

7.1 Design and printing for degree of conversion test

Each experimental group was prepared in accordance with same method as in section 4. The prepared 3D printed resins were ground using a Mini Mill (Pulverisette 23; Fritsch GmbH, Idar-Oberstein, Germany). The powder of each experimental resin was mixed with KBr powder at a ratio of 1:100. The resulting mixture was placed into a disk-shaped mold and compressed using a hydraulic press to produce specimens in the form of transparent pellets.

7.2. Degree of conversion analysis

Fourier-transform infrared spectroscopy (FT-IR) spectra were recorded using an FT-IR spectrometer (VERTEX 70; Bruker, Billerica, USA). The polymerized 3D printing resin was performed in transmission mode, while the uncured 3D printing resin was performed in attenuated total reflectance mode. The spectra were obtained in the range of 4000 to 400 cm^{-1} with a total of 16 scans per spectrum and a resolution of 4 cm^{-1}.

All spectrums were referenced to the aromatic C=C bonds at 1608 cm^{-1}, and the degree of conversion of each specimen was determined by comparing the intensity of the aliphatic C=C stretching vibration at 1638 cm^{-1} of the polymerized 3D printing resin and uncured 3D printing resin. The degree of conversion (DC) was determined according to the following equation:

$$DC\ (\%) = \left[1 - \frac{(1638cm^{-1}/1608cm^{-1})cured}{(1638cm^{-1}/1608cm^{-1})uncured}\right] \times 100$$

8. Dimensional accuracy of 3D printed specimens

8.1. Design and printing for dimensional accuracy test

The 3D printing accuracy specimen (n=6) was prepared in the shape of a die based on Figure 7. Specimen preparation was performed in the same method as in section 4.

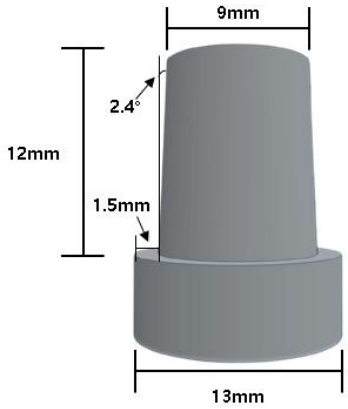

Figure 7. Specimen design for dimensional accuracy test.

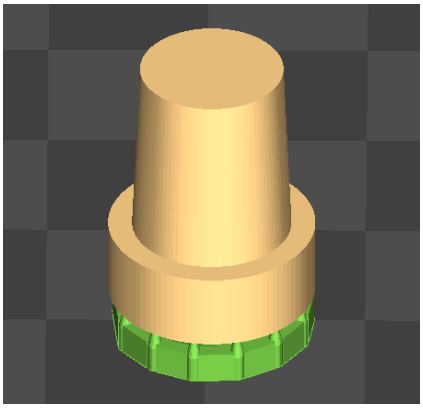

Figure 8. STL image of the specimen for dimensional accuracy test, displaying the designed specimen (yellow) and the support structure (green) for 3D printing.

8.2. Evaluation for dimensional accuracy

The fabricated specimens were scanned with a light model scanner (Medit T710; Medit, Seoul, Korea) on the surface. Dimensional accuracy between the original STL file and different experimental groups was compared through best-fit alignment using 3D inspection software (Geomagic Control X; 3D Systems, Rock Hill, SC, USA). Afterward, 2D analysis was performed by equally dividing the superimposed data vertically. The maximum and minimum range were set at ± 0.5 mm, and tolerance levels were set at ± 0.05 mm. Each specimen was measured three times as shown in Figure 9, and the average value was calculated and used.

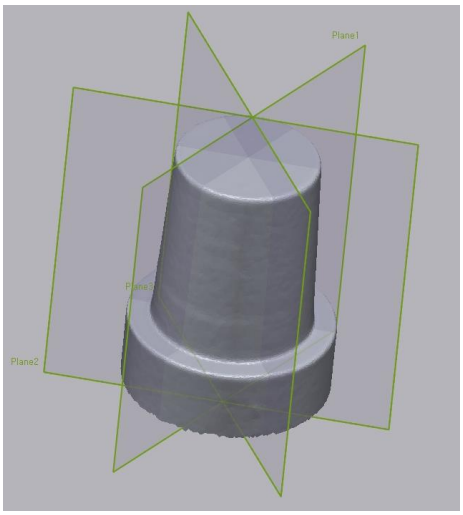

Figure 9. Plane division for 2D analysis.

9. Cytotoxicity

To evaluate the cytotoxic effects of experimental 3D printed resin, a cytotoxicity test was carried out by using the 3-(4,5-dimethylthiazol-2-yl)-2,5-diphenyltetrazolium bromide (MTT) assay according to the ISO 10993-5:2009 standard (ISO, 2009).

9.1. Preparation of cell culture

The L-929 mouse fibroblasts were cultured in RPMI-1640 cell culture medium (Welgene, Gyeongsangbuk-do, Korea) containing 10 % fetal bovine serum (FBS; Gibco, Grand Island, NY, USA) and 1 % penicillin streptomycin (Gibco, Grand Island, NY, USA). The cell suspension was prepared at a concentration of 1×10^5 cell/ml and inoculated onto 96-well cell culture plates (100 μl/well). The multi-well plates were incubated at 37 ℃, with 5 % CO_2 in air for 24 h.

9.2. Extracts of 3D printed specimens

The specimens for the cytotoxicity test were in the form of cubes with dimensions of 10 × 10 × 10 mm. Specimen preparation was performed in the same method as in section 4. The residual supporters of 3D printed specimens were polished to #1000 grit silicon carbide paper.

Following the ISO standard 10993-12:2012 (ISO, 2012), the extract was prepared by soaking specimens in culture medium RPMI-1640 at a concentration of 3 cm^2/mL. The extraction was carried out at 37 ℃ for 24 h.

9.3. Methylthiazol tetrazolium (MTT) assay

The blank control group used RPMI-1640 eluted at 37 ℃ for 24 h. The positive control group used 1 % phenol (Sigma-Aldrich, Steinheim, Germany). The negative control group used high-density polyethylene film (Hatano Research Institute, Ochiai, Japan). The medium of the cultured L-929 cells was then replaced by equal volumes (100 μl) of the extracts and incubated at 37 ℃, 5% CO_2 in air for 24 h.

Following removal of the test extracts, 50 μl MTT solution with a concentration of 1 mg/mL was added to each well and incubated in a dark environment for 2 h at 37 ℃. MTT solution was removed and 100 μl dimethyl sulfoxide (DMSO; Duksan reagents, Ansan, Korea) was added to each well. The DMSO-treated plate was shaken with a rotator (C-SKS; Changshin Science, Seoul, Korea) for 30 min. The absorbance at 570 nm was measured using a microplate spectrophotometer (Epoch; Biotek, Winooski, USA). The cell viability was calculated using the following equations:

$$\text{Viab.}\,\% = \frac{100 \times OD_{570e}}{OD_{570b}}$$

Where, OD_{570e} is the value of the measured optical density of the extracts of the test sample, OD_{570b} is the value of the measured optical density of the blank.

10. Statistical analysis

To evaluate the characteristics of the 3D printing resin with surface-treated zirconia fillers, mechanical properties, water sorption and solubility, degree of conversion, dimensional accuracy, and cytotoxicity data were analyzed using one-way ANOVA followed by Tukey's statistical test. The within-group comparisons of flexural strength and modulus based on storage conditions were conducted using an independent samples *t*-test. All statistical analyses were performed using the SPSS 25 software program (IBM, Armonk, NY, USA). The all statistical significance levels were set at a confidence 95 %.

III. RESULTS

1. Characterization of zirconia surface treated with 10-MDP

1.1. Morphology

TEM images of zirconia filler and surface-treated zirconia filler are shown in Figure 10. No organic compounds were observed on the surface of the zirconia. However, the surface-treated zirconia showed some organic compounds in the 1D group. A greater amount of organic compounds is observed in the 7D and 14D groups compared to the 1D group.

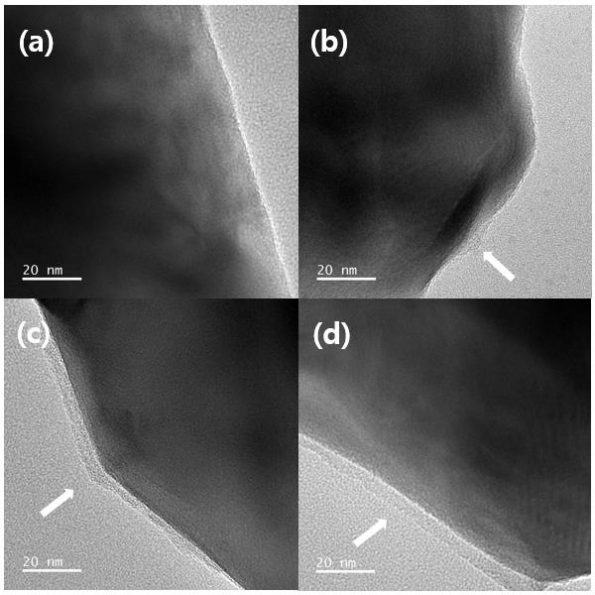

Figure 10. TEM images of zirconia fillers with different exposure times for surface treatment: (a) zirconia, (b) 1D, (c) 7D, (d) 14D.

1.2. Measurement of 10-MDP surface teatment quantity on zirconia fillers

The TGA results of surface-treated zirconia fillers for different times are presented in Figure 11. Neat zirconia fillers showed no change in weight. The percentage weight losses of the surface-treated zirconia fillers were 0.8 wt.% in the 1D group, 1.25 wt.% in the 7D group, and 1.4 wt.% in the 14D group.

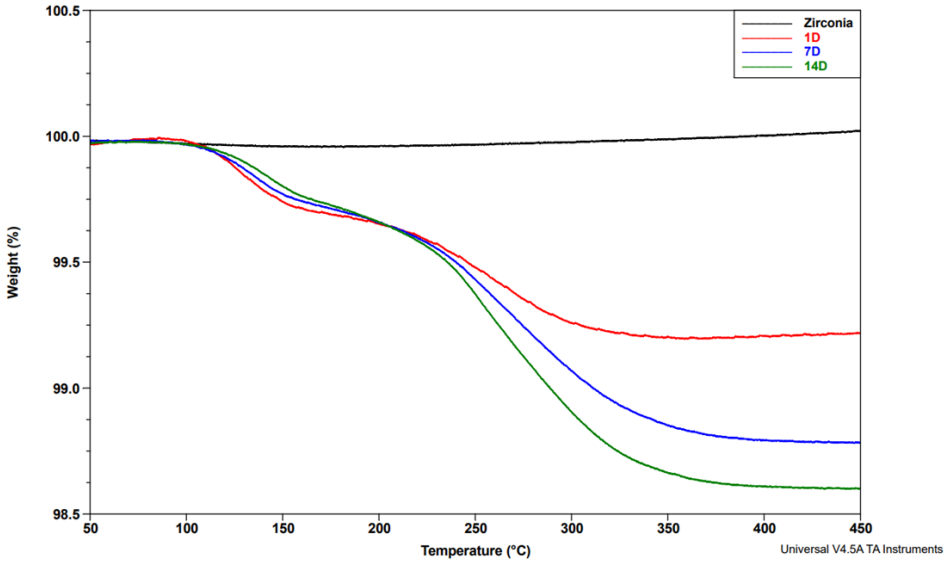

Figure 11. Thermogravimetric analysis of zirconia fillers surface-treated with 10-MDP. The black, red, blue, and green lines represent the results for untreated, 1 day, 7 days, and 14 days surface-treated zirconia fillers, respectively.

1.3. Chemical property

The XPS O1s spectra (525-540 eV) and corresponding peak fitting results are shown in Figure 12. The percent of each peak was calculated from the relative peak area in the XPS O1s spectrum. The component peak centered at ~530 eV is assigned to the Zr-O-Zr bond. The component peak centered at ~531.5 eV is assigned to the P-O-Zr bond. The component peak centered at ~532.9 eV is assigned to the P-OH/C-O bond. Based on the peak areas, the relative content of chemical bonds was as follows: 1D group, Zr-O-P bond was 25.03 %, Zr-O-Zr bond was 48.42 %, and P-OH/C-O bond was 26.55 %. 7D group, Zr-O-P bond was 32.27 %, Zr-O-Zr bond was 47.65 %, and P-OH/C-O bond was 20.08 %. 14D group, Zr-O-P bond was 42.92 %, Zr-O-Zr bond was 20.58 %, and P-OH/C-O bond was 36.50 %.

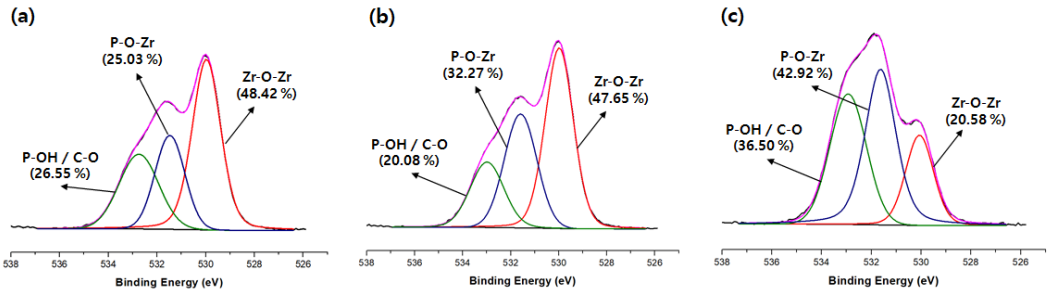

Figure 12. X-ray photoelectron spectroscopy of O1s spectra for zirconia fillers with different exposure times for surface treatment: (a) 1D, (b) 7D, (c) 14D.

2. Mechanical Properties of 3D Printing C&B Resin Incorporating Zirconia Fillers

2.1. Flexural strength

Figure 13 displays the results of the flexural strength of specimens based on storage conditions.

The flexural strength of specimens stored at room temperature (dry condition) was (102.6 ± 4.7) MPa for the control group, (86.5 ± 3.3) MPa for the 0D group, (100.6 ± 9.3) MPa for the 1D group, (123.7 ± 6.2) MPa for the 7D group, and (130.2 ± 6.3) MPa for the 14D group. The 0D group exhibited significantly the lowest flexural strength ($p < 0.05$). No significant difference was observed between the control group and the 1D group ($p > 0.05$). Although there was no significant difference between the 14D group and the 7D group ($p > 0.05$), their results were significantly higher than those of the other groups ($p < 0.05$).

The flexural strength of specimens immersed in water (wet condition) was (108.7 ± 5.5) MPa for the control group, (88.2 ± 4.5) MPa for the 0D group, (86.5 ± 9.0) MPa for the 1D group, (118.0 ± 5.0) MPa for the 7D group, and (118.0 ± 6.8) MPa for the 14D group. There was no significant difference between the 0D group and the 1D group ($p > 0.05$), both of which showed significantly the lowest flexural strength ($p < 0.05$). The 14D group showed significantly the highest flexural strength ($p < 0.05$), and no significant difference was observed compared to the 7D group ($p > 0.05$).

Comparisons were made within the same group based on storage conditions. Significant differences in flexural strength were observed among all groups except for the 0D group ($p < 0.05$).

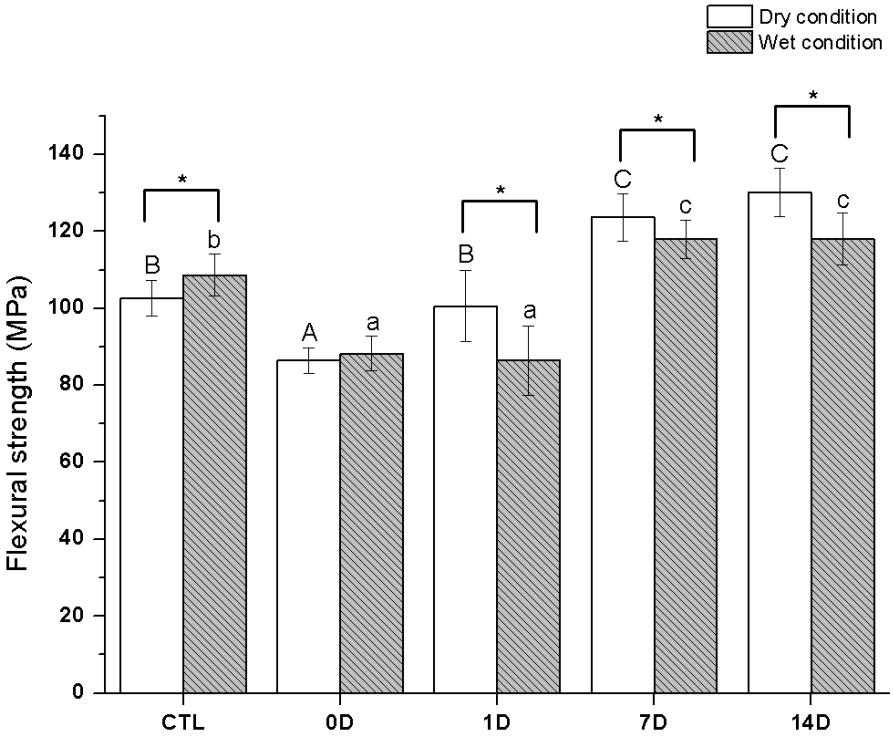

Figure 13. Flexural strength of each group according to storage conditions. Uppercase letters above the bar graph indicate significant differences among specimens under dry conditions, while lowercase letters indicate significant differences among specimens under wet conditions ($p < 0.05$). Asterisks (*) denote significance for comparisons between storage conditions within each group, as analyzed by paired *t*-test ($p < 0.05$).

2.2. Flexural modulus

Figure 14 displays the results of the flexural modulus of specimens based on storage conditions.

The flexural modulus of specimens stored at room temperature was (3065 ± 101) MPa for the control group, (2678 ± 53) MPa for the 0D group, (2757 ± 109) MPa for the 1D group, (4032 ± 197) MPa for the 7D group, and (4160 ± 198) MPa for the 14D group. The flexural modulus of specimens immersed in water was (3278 ± 172) MPa for the control group, (2667 ± 108) MPa for the 0D group, (2439 ± 119) MPa for the 1D group, (3797 ± 214) MPa for the 7D group, and (3770 ± 278) MPa for the 14D group. The specimens under dry and wet conditions exhibited similar trends in flexural modulus. There were no significant differences between the 0D and 1D groups ($p > 0.05$), both of which showed significantly lower flexural modulus ($p < 0.05$). The 14D group showed no significant difference from the 7D group ($p > 0.05$), but exhibited a significant difference from the control group ($p < 0.05$).

Comparisons were made within the same group based on storage conditions. Significant differences in flexural modulus were observed among all groups except for the 0D group ($p < 0.05$).

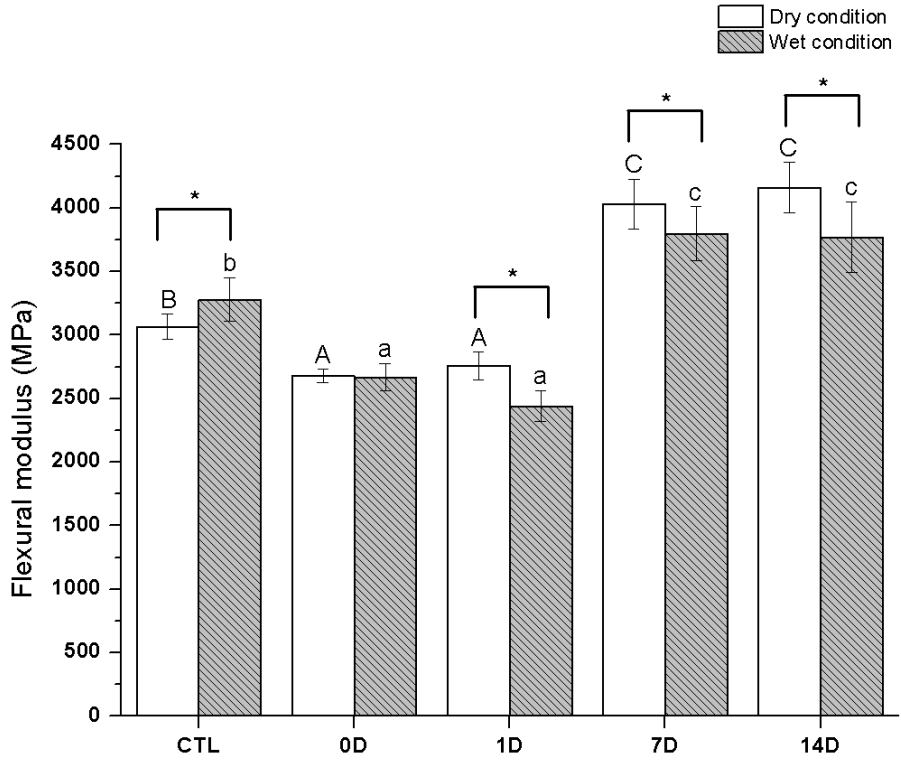

Figure 14. Flexural modulus of each group according to storage conditions. Uppercase letters above the bar graph indicate significant differences among specimens under dry conditions, while lowercase letters indicate significant differences among specimens under wet conditions ($p < 0.05$). Asterisks (*) denote significance for comparisons between storage conditions within each group, as analyzed by paired *t*-test ($p < 0.05$).

2.3. Fractured surface analysis

The SEM images of the fractured surface of the 3D-printed resin are shown in Figure 15. The fractured surfaces of the other groups were rough surfaces than that of the control group. The fractured surface of the resin containing neat zirconia filler revealed voids where the filler had been. In contrast, the fractured surface of the resin with added surface-treated zirconia filler showed a distinct reduction in voids. As indicated by the white arrows, the 0D group showed a tendency for separation between the zirconia filler and the resin matrix interface upon fracture, while the surface-treated zirconia containing group exhibited fracture within the resin or zirconia filler.

From the EDS mapping results in Figure 16, the zirconium element was confirmed, indicating that zirconia fillers were mixed and dispersed into the 3D printing resin. Additionally, for the zirconia fillers surface-treated with 10-MDP, the phosphorus element was further detected.

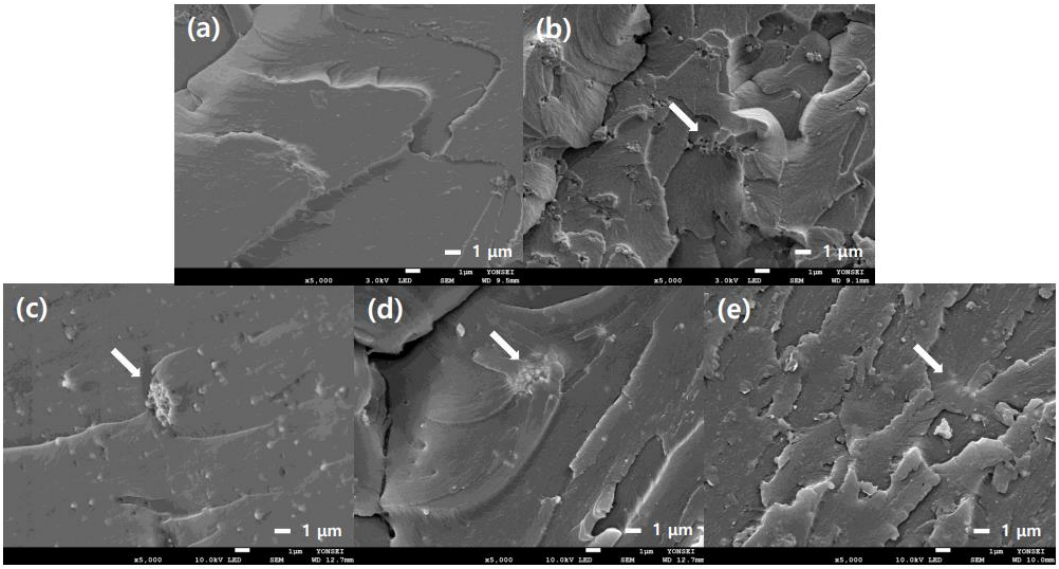

Figure 15. SEM images of the fractured surface of 3D-printed resin with added zirconia filler or surface-treated zirconia filler: (a) CTL, (b) 0D, (c) 1D, (d) 7D, (e) 14D.

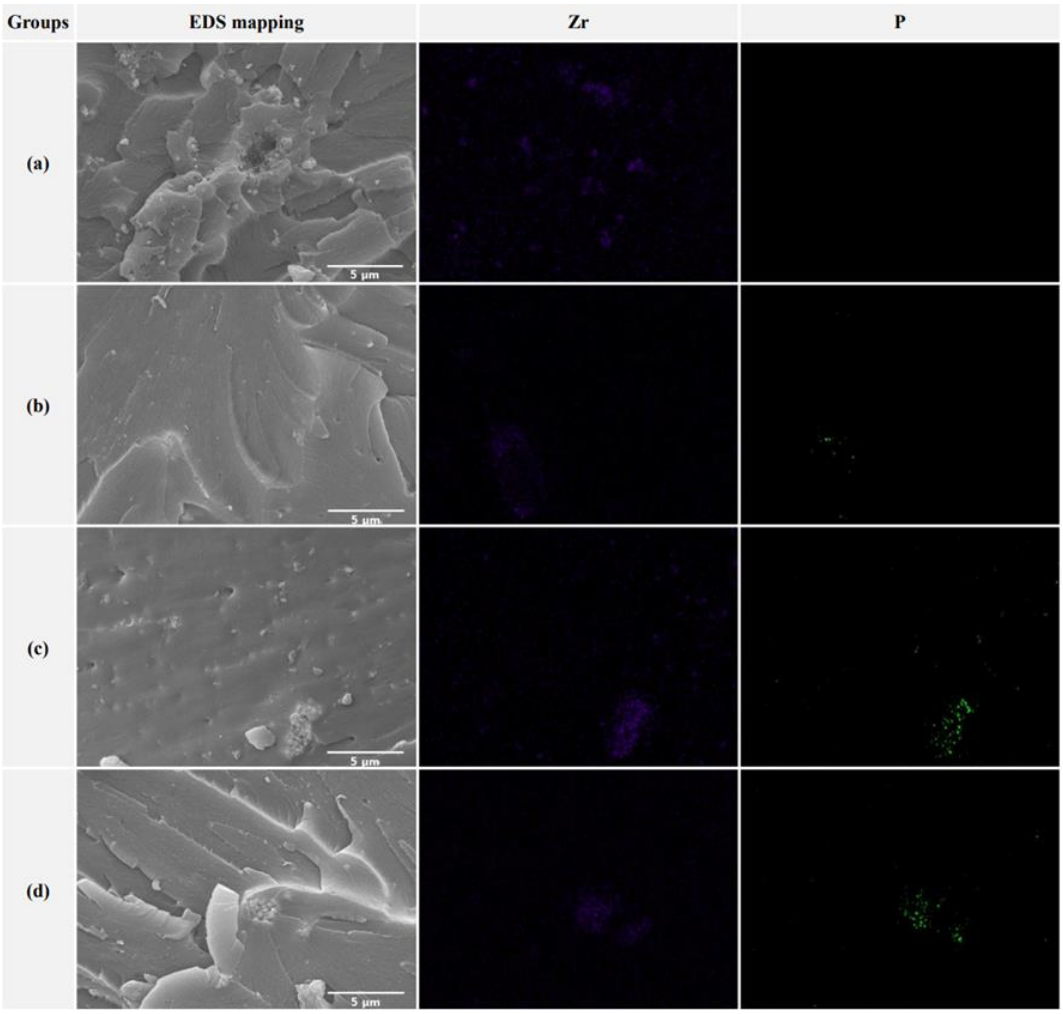

Figure 16. EDS mapping images of the fractured surface of 3D-printed resin with added zirconia filler or surface-treated zirconia filler: (a) 0D, (b) 1D, (c) 7D, (d) 14D.

2.4. Microhardness

The results of the Vickers hardness test are shown in Figure 17. The hardness values of each group were control group (13.36 ± 0.93), 0D group (15.35 ± 0.83), 1D group (16.15 ± 0.45), 7D group (16.09 ± 0.62), and 14D group (16.43 ± 0.79). Compared to the control group, all experimental groups with added zirconia showed significantly higher results ($p < 0.05$). The 0D group showed significantly lower results compared to the 14D group ($p < 0.05$).

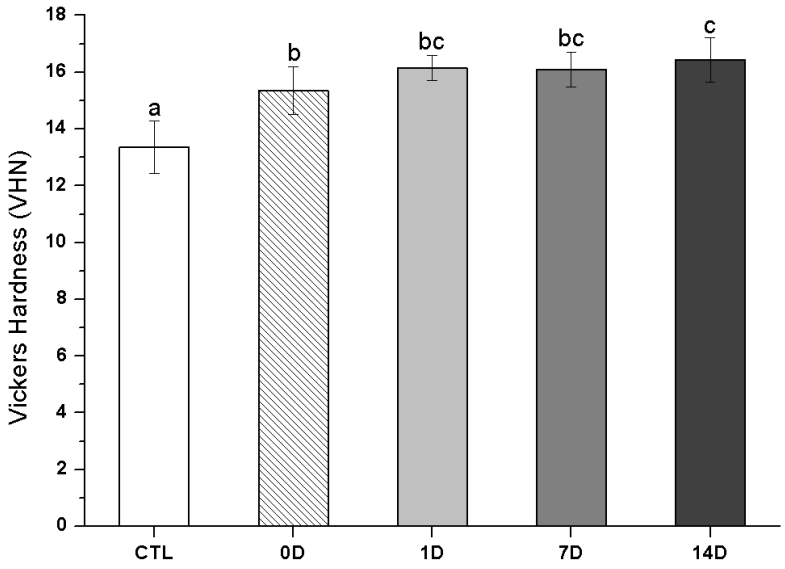

Figure 17. Microhardness of each group. Each value represents the mean of measurements, and the error bars represent the standard deviation of the mean (mean ± standard deviation). Same lowercase letter in the same column indicates no significant difference ($p > 0.05$).

3. Water sorption and solubility

The results of water sorption and solubility are shown in Table 3. In the results of water sorption, the control group showed significant differences with the 7D and 14D groups ($p < 0.05$), but no significant differences were observed with the 0D and 1D groups ($p > 0.05$). In results of water solubility, the control group showed significant differences with the 1D, 7D, and 14D groups ($p < 0.05$), but no significant difference was observed with the 0D group ($p > 0.05$).

Table 3. Water sorption and solubility of each group

Groups	Water sorption (μg/mm^3)	Solubility (μg/mm^3)
CTL	17.15 ± 0.66 ^{b}	1.32 ± 0.71 ^{a}
0D	16.31 ± 0.91 ^{ab}	2.12 ± 0.58 ^{ab}
1D	16.04 ± 0.77 ^{ab}	2.17 ± 0.60 ^{b}
7D	15.94 ± 1.29 ^{a}	2.14 ± 0.71 ^{b}
14D	15.78 ± 0.55 ^{a}	2.22 ± 0.54 ^{b}

Same lowercase letter in the same column indicates no significant difference ($p > 0.05$).

4. Degree of conversion

The results of the degree of conversion are shown in Figure 18. The degree of conversion result values were (68.94 ± 2.38) % for the control group, (68.48 ± 0.53) % for the 0D group, (70.68 ± 0.33) % for the 1D group, (70.30 ± 0.64) % for the 7D group and (70.00 ± 0.92) % for the 14D group. The experimental group with surface-treated zirconia added showed higher results compared to the control group. However, no significant differences were observed among all groups ($p > 0.05$).

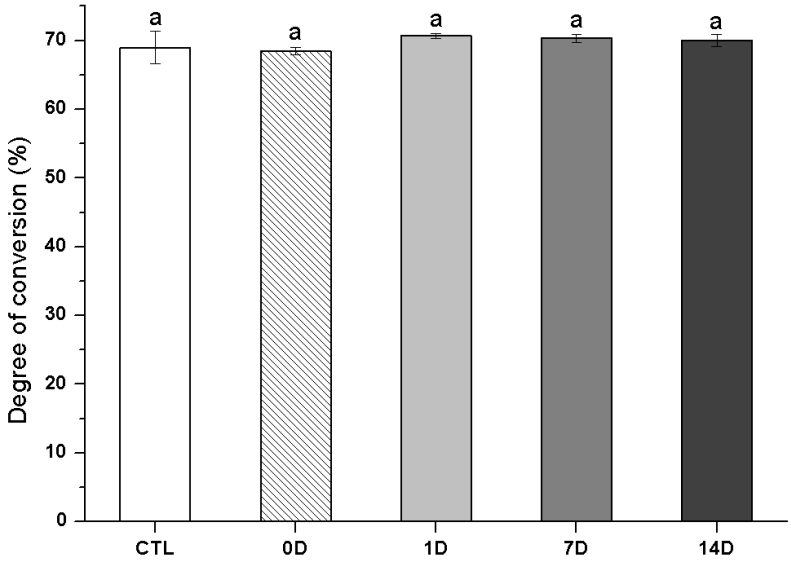

Figure 18. Degree of conversion of each group. Each value represents the mean of measurements, and the error bars represent the standard deviation of the mean (mean ± standard deviation). Same lowercase letter in the same column indicates no significant difference ($p > 0.05$).

5. Dimensional accuracy of 3D printed specimens

The 2D analysis using the color difference map was shown in Figure 19. The experimental groups were displayed on the color map in comparison to the original STL file. In all groups except the control group, green lines were observed on both the Z-axis and XY-axis. The control group exhibited green lines on the Z-axis and blue lines on the XY-axis.

The results of dimensional accuracy are detailed in Table 4. The accuracy on the XY-axis showed the deviation from the true value in the control group, demonstrating significantly lower accuracy compared to all other groups ($p < 0.05$). There were no significant differences among all groups except for the control group ($p > 0.05$). However, all groups were within the clinically acceptable tolerance levels.

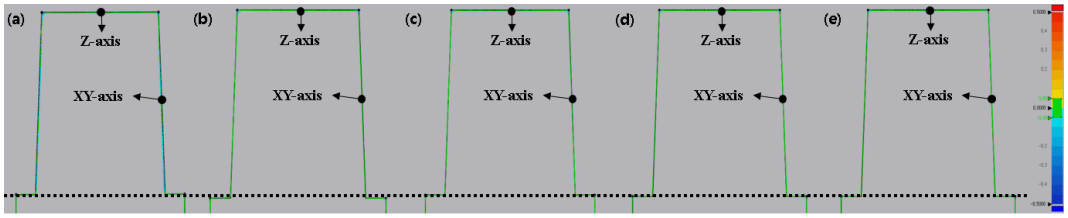

Figure 19. 2D analysis of accuracy by using a colour difference map (green represents good fit, yellow or red represents positive error, and blue represents negative error): (a) CTL group, (b) 0D group, (c) 1D group, (d) 7D group, (e) 14D group. The black dashed line shows the base plane.

Table 4. Mean and standard deviation of dimensional accuracy

Groups	Z-axis (μm)	XY-axis (μm)
CTL	- 35.85± 6.70 [a]	- 35.29 ± 9.54 [a]
0D	- 32.22 ± 5.99 [a]	7.74 ± 9.09 [b]
1D	- 35.73 ± 4.98 [a]	- 3.27 ± 8.04 [b]
7D	- 33.22 ± 6.48 [a]	0.09 ± 3.67 [b]
14D	- 37.10 ± 2.98 [a]	- 3.93 ± 4.71 [b]

Same lowercase letter in the same column indicates no significant difference ($p > 0.05$). Different lowercase letters in the Z-axis and XY-axis columns indicate a significant difference between groups ($p < 0.05$)

6. Cytotoxicity

The results of the cytotoxicity test are shown in Figure 20, which revealed no significant differences among the tested groups ($p > 0.05$). The cell viability values were as follows: (5.34 ± 0.24) % for the positive control, (90.24 ± 4.04) % for the negative control, (77.33 ± 6.32) % for the control group, (82.19 ± 3.92) % for the 0D group, (75.37 ± 3.79) % for the 1D group, (80.04 ± 2.69) % for the 7D group, and (80.62 ± 5.94) % for the 14D group, in comparison to the blank.

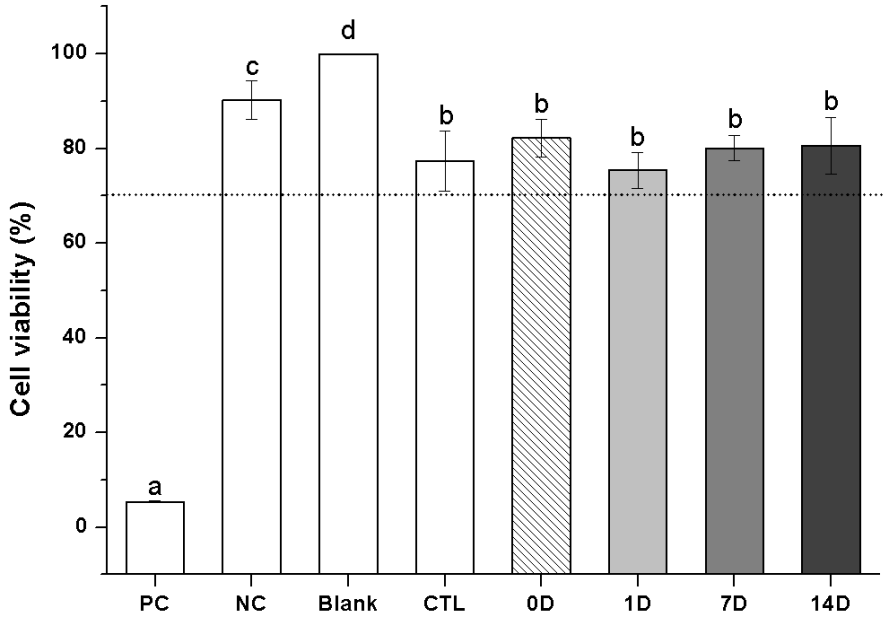

Figure 20. Cell viability of each group. The dotted line represents the minimum ISO standard criterion: cell viability less than 70% is considered cytotoxic. Each value represents the mean of measurements, and error bars represent the standard deviation of the mean (mean ± standard deviation). Differences in lowercase alphabetical letters above the bar graph indicate significant differences among the groups ($p < 0.05$).

IV. DISCUSSION

For the fabrication of fixed dental prostheses, the mechanical properties, physical properties, conversion rate, accuracy, and biocompatibility of 3D printing resin are crucial. Particularly, due to the necessity of withstanding occlusal forces, research to enhance mechanical properties for clinical application was required. Zirconia fillers offer various advantages such as superior mechanical properties, biocompatibility, and excellent wear resistance. However, zirconia fillers lack chemical affinity with silane coupling agents. It was expected that surface treatment of zirconia filler with 10-MDP, which has a chemical affinity with zirconia, would modify the zirconia surface. Surface treatment was conducted with different exposure times based on previous studies (Chen et al., 2017b; Wu et al., 2019; Yang et al., 2020).

This study investigated the addition of 10-MDP surface-treated zirconia fillers to 3D printing crown & bridge resin to evaluate its properties. The particle size analysis of the zirconia powder used in this study showed that the D50 was 537.9 nm. First, to confirm the surface treatment of the zirconia fillers, TEM, TGA, and XPS analyses were conducted. Second, the characteristics of the 3D printing resin with surface-treated zirconia fillers were examined by assessing mechanical properties, water sorption and solubility, dimensional accuracy, degree of conversion, and cytotoxicity.

TEM images were taken to verify the modification on the surface of zirconia. In Figure 10a, it was observed that there are no organic materials on the surface of zirconia, and it appears clean. In Figure 10b, unlike Figure 10a, small amounts of non-uniform organic compounds are observed on some parts of the zirconia surface. Organic compounds with a thickness of approximately 5 nm were confirmed in Figures 10c and 10d, observed over a wider range compared to the organic compounds observed in Figure 10b. The organic compound observed in the TEM images is presumed to be composed of 10-MDP, as evidenced by the presence of Zr-O-P and P-OH/C-O bonds in the XPS results of Figure 12, and the detection of phosphorus element in the EDS results of Figure 16 for the zirconia

fillers surface-treated with 10-MDP. These results were similar to references in which zirconia fillers were surface treated with MDP-containing agents used for conditioning (Yang et al., 2020).

TGA measurements were conducted to assess the increase in organic compounds treated on zirconia according to the surface treatment time. According to the TG curve, the weight loss in the temperature range of 100°C to 450°C is attributed to the decomposition of organic compounds. The 1D group showed a decrease of 0.8 wt.%, the 7D group showed a decrease of 1.25 wt.%, and the 14D group showed a decrease of 1.4 wt.%. In the reference studies, surface treatment of zirconia powder was carried out by adding 10-MDP to the primer at varying concentrations. The TGA results showed a weight loss of 0.51 wt.%. In the present study, it was observed that a greater amount was surface treated, which is expected to be due to differences in the surface treatment method.

The XPS measurements were conducted to confirm the presence of 10-MDP bound to modified zirconia fillers. When zirconia is chemically bonded with 10-MDP, Zr-O-Zr, Zr-O-P, and P-OH/C-O groups can be observed (Wu et al., 2019; Yang et al., 2020). Zr-O-Zr represents the zirconia, and Zr-O-P indicates the chemical bonding between the phosphate group of 10-MDP and zirconia. P-OH/C-O represents the methyl methacrylate and carbon structures, as well as the phosphate structure present in 10-MDP. The Zr-O-P, which indicates the chemical bonding between zirconia and 10-MDP, was observed to gradually increase with the surface treatment time.

Based on the results from TEM, TGA, and XPS analyses, it was confirmed that 10-MDP was successfully surface-treated onto the zirconia fillers. Additionally, it was observed that the exposure time of surface treatment affects the modification of the zirconia fillers.

3D printed resin needs to have appropriate mechanical properties because the 3D printed restoration can encounter mechanical stresses when placed on areas that are subjected to force of mastication (Dejak et al., 2003). The mechanical properties of the resin depend on the resin matrix, degree of conversion and the presence of filler (Gonçalves et al., 2009;

Rodríguez et al., 2019). In this study, the resin matrix used a commercially available 3D-printed crown and bridge resin and incorporated a surface-treated zirconia filler. According to ISO 4049:2019 (ISO, 2019), flexural strength should be measured after storage in wet conditions. However, in this study, to determine whether the 3D printing resin with 10-MDP surface-treated zirconia fillers exhibited differences in flexural strength and modulus depending on the presence or absence of immersion, experiments were conducted under two conditions (wet and dry). The ISO 4049:2019 (ISO, 2019) standard requires a minimum 100 MPa of flexural strength. Figure 13 reveals that under dry conditions, the flexural strength exceeded 100 MPa for all groups except the 0D group. The 0D group showed a significantly lower value at 86.5 MPa. These results align with previous studies indicating that untreated zirconia, unable to form a chemical bond with the resin matrix, compromises flexural strength (Zidan et al., 2021). Additionally, the image in Figure 15b reveals numerous voids. This indicates the absence of chemical bonding between the zirconia filler and the resin, resulting in their separation at the interface. The 1D group exhibited flexural strength results similar to those of the control group. Figure 10b indicates partial binding of 10-MDP to the surface of zirconia, suggesting bonding between zirconia and resin. Figure 15 reveals that in the 1D, 7D, and 14D groups, unlike the 0D group, there are very few voids, indicating fracture within the resin or aggregated zirconia fillers. Moreover, the 7D and 14D groups showed an increasing trend in flexural strength with increasing surface treatment time.

Under wet conditions, the 0D group exhibited results similar to those of the dry condition group. The 1D group showed results similar to the 0D group, unlike under dry conditions. It was also observed that the flexural strength in the 7D and 14D groups was significantly lower compared to that under dry conditions ($p < 0.05$). Water molecules are able to penetrate between polymer chains. The interface between the particle and polymer is water-sensitive because of the high surface energy of the particle related to the polymer, and the permeability of the polymer allows water to reach the interface (Asopa et al., 2015). For silanized silica fillers, water infiltration initiates the hydrolysis of silane at the filler–

polymer interfaces, thereby acting as the threshold for filler debonding (Araújo-Neto et al., 2021; Van Landuyt et al., 2010). According to previous studies, 10-MDP can be hydrolyzed into substances such as metasylic acid, decane-diol, and phosphoric acid (Teshima, 2010). The wet conditions are presumed to have influenced the performance of 10-MDP, leading to a weakened bond between the filler and the resin matrix.

The flexural modulus exhibited a similar trend to flexural strength. The surface-treated groups showed an increase in flexural modulus, but the 1D group showed no significant difference from the 0D group ($p > 0.05$). No significant difference was observed when the surface treatment time was longer than 7 days ($p > 0.05$). In Figure 18, all groups showed no significant difference in the degree of conversion ($p > 0.05$). Therefore, the increase in flexural strength and modulus indicates the influence of surface-treated zirconia fillers.

Figure 17 showed that all experimental groups exhibited significantly higher microhardness results compared to the control group. According to research, the addition of modified nano-zirconia fillers to PMMA composites has been shown to increase hardness (Ergun et al., 2018). Furthermore, after incorporating salinized zirconia NPs in acrylic resin, there was a significant increase in hardness and a minor improvement in surface roughness (Ali Sabri et al., 2021).

Most researchers have suggested that water sorption, solubility, and related diffusion coefficient of the dental composite are influenced by the chemistry of the resin matrices, the rate of polymerization, the size and distribution of filler particles, and the interfacial bonding between the filler and resin matrix (Beatty et al., 1998; Calais and Soderholm, 1988; Ferracane, 1994). In the current study, since all specimens had the same matrix, differences in water sorption and solubility between materials may be attributed to variations in filler morphology and associated interfacial bonding. Additionally, due to the addition of zirconia fillers, the amount of resin matrix decreases, which may result in lower water sorption values (Randolph et al., 2016). According to previous studies, it has been

observed that water absorption decreases with increasing concentrations of silanized zirconia filler (Aati et al., 2021).

When the resin specimens are immersed in water, the unreacted monomer may dissolve and be leached out of the specimens (Tuna et al., 2008). These result in loss of weight and can be measured as solubility. Therefore, the water sorption and solubility may affect the initial dimensional change of resin, the clinical performance, and the biocompatibility (Toledano et al., 2003). The solubility was the lowest in the control group ($p < 0.05$), with no significant difference observed compared to the 0D group ($p > 0.05$). The groups with surface-treated zirconia filler added showed higher solubility compared to the control group ($p < 0.05$), which may have contributed to the partial hydrolysis and dissolution of some of the 10-MDP attached to the zirconia filler. The ISO 4049:2019 (ISO, 2019) standard requires the following maximum values: water sorption ≤ 40 μg/mm^3 and solubility ≤ 7.5 μg/mm^3. All groups satisfied the ISO 4049 standard for water sorption and solubility values.

Degree of conversion is the important factor in resin materials. This is because it can affect mechanical and physical properties and cytotoxicity (Eshmawi et al., 2018; Fujioka-Kobayashi et al., 2019; Lin et al., 2020). Figure 18 reveals that there is no significant difference in the degree of conversion between the control group and the other groups ($p > 0.05$). This indicates that the addition of zirconia fillers in 3D printing resin does not affect the polymerization mechanism.

Low accuracy can lead to problems such as the need for chairside adjustment or compromised longevity of the restoration (Park et al., 2020). The accuracy of the printed objects is correlated to the front polymerization kinetics of formulated resins (Vitale and Cabral, 2016). Dental resins form a dense polymer network through the polymerization process, which causes volumetric contraction or shrinkage (Acosta Ortiz et al., 2015). Table 4 demonstrates that no significant differences were observed among all groups in the Z-axis. In the XY-axis, all experimental groups showed values significantly closer to the true

values compared to the control group. However, all groups are within the acceptable tolerance levels, making them clinically usable. DLP printing polymerizes the resin by exposing it to UV light. When zirconia fillers and dental monomers are combined, light scattering occurs because of the large difference in refractive indexes between zirconia and the monomers (Mizobuchi et al., 2024). This scattering occurs when UV light propagates through the 3D printing resin and zirconia fillers, potentially resulting in a cured area larger than the original STL size. (Liu et al., 2024). Therefore, the addition of zirconia filler complements resin shrinkage and helps adjust the accuracy of 3D printed objects.

The cytotoxicity of all groups was assessed following the guidelines outlined in ISO 10993-5:2009 (ISO, 2009). No significant differences were observed among the groups, and since the cell viability was over 70%, no cytotoxicity was observed according to the ISO standard. The residual monomers and additives are free to diffuse out from the cured materials. They may be released into surrounding tissues and may have potential toxic effects (Chang et al., 2015). The results of the degree of conversion showed no significant differences among all groups. This suggests that since the polymerization reaction of all groups is similar, the amount of unreacted monomer released is expected to be similar as well. The 3D printing resin has been augmented with zirconia fillers. It is widely acknowledged in the literature that zirconia fillers typically exhibit excellent biocompatibility (Alshamrani et al., 2023; Bannunah, 2023). According to previous studies, the cytotoxicity profile of 10-MDP was suggested to be most likely caused to its acidic nature (Upson et al., 2023). However, since 10-MDP was treated on the surface of the zirconia filler, it does not exhibit an acidic nature, and the amount of 10-MDP present in the 3D printing resin was very small. Therefore, 10-MDP is not expected to affect cytotoxicity.

A limitation of this study is that the flexural strength of 3D printing resin with surface-treated zirconia fillers decreased in a wet condition. Further research is needed to identify the exact cause.

Surface treatment of zirconia fillers with 10-MDP increases the flexural strength. However, the amount of 10-MDP chemically bonded to zirconia is very small. Further research aimed at increasing the bonding between zirconia and 10-MDP could further enhance the mechanical properties.

V. CONCLUSION

In the current research, zirconia fillers were surface-treated with 10-MDP, with variations in surface treatment time. 3D printing crown & bridge resin containing surface-treated zirconia fillers was manufactured, and its mechanical properties, water sorption and solubility, degree of conversion, dimensional accuracy, and cytotoxicity were evaluated to investigate its potential clinical application. Within the laboratory conditions of this study, the following results and conclusions were drawn:

1. According to the TEM, TGA, and XPS results, 10-MDP was demonstrated to successfully treat the surface of the zirconia fillers. Furthermore, it was observed that the amount of 10-MDP attached to the zirconia surface increased as the surface treatment time increased.

2. The flexural strength in the 0D group was consistently the lowest regardless of the storage conditions, with the 7D and 14D groups showing significantly higher values than the other groups ($p < 0.05$). In terms of flexural modulus according to storage conditions, the 0D and 1D groups showed significantly lower results compared to other groups, while the 7D and 14D groups exhibited significantly higher results than the control group ($p < 0.05$). In terms of microhardness, the control group showed significantly lower values, while the 14D group showed significantly higher results ($p < 0.05$). As a result, the null hypothesis that there is no significant difference in the mechanical properties of 3D printing resin groups containing modified zirconia fillers with various surface treatment times using 10-MDP was rejected.

3. In the water sorption test, the control group showed the highest results, while the 14D group showed the lowest ($p < 0.05$). However, in the water solubility test, the control group exhibited the lowest results compared to the groups with added surface-treated zirconia fillers ($p < 0.05$). As a result, the null hypothesis that there is no significant difference in the water sorption and solubility of 3D printing resin groups containing modified zirconia fillers with various surface treatment times using 10-MDP was rejected.

4. The degree of conversion did not show significant differences in all groups ($p > 0.05$). Therefore, the null hypothesis that there is no significant difference in the degree of conversion of 3D printing resin groups containing modified zirconia fillers with various surface treatment times using 10-MDP was accepted.

5. In terms of dimensional accuracy, the results of the XY-axis accuracy were significantly closer to the true value in the groups with added zirconia fillers compared to the control groups ($p < 0.05$). There were no significant differences observed in the Z-axis among all groups ($p > 0.05$). Therefore, the null hypothesis that there is no significant difference in the dimensional accuracy of 3D printing resin groups containing modified zirconia fillers with various surface treatment times using 10-MDP was rejected.

6. There were no significant differences in cytotoxicity among all groups ($p > 0.05$). Therefore, the null hypothesis that there is no significant difference in the cytotoxicity of 3D printing resin groups containing modified zirconia fillers with various surface treatment times using 10-MDP was accepted.

In conclusion, surface treatment of zirconia filler with 10-MDP was found to be feasible, and differences were observed among the groups based on the exposure times for surface treatment. Additionally, the addition of surface-treated zirconia fillers was shown to influence the properties of 3D printing resin.

The 14D group and the 7D group showed similar experimental results. Therefore, it is considered that the optimum exposure time for surface treatment is 7 days. Additionally, surface-treated zirconia fillers with 10-MDP incorporated into 3D printing resin exhibited no cytotoxicity and demonstrated the potential to enhance mechanical properties without adversely affecting dimensional accuracy. Therefore, the surface-treated zirconia fillers with 10-MDP can be sufficiently utilized as fillers for dental 3D printing resins.

REFERENCES

Aati S, Akram Z, Ngo H, Fawzy AS: Development of 3D printed resin reinforced with modified ZrO_2 nanoparticles for long-term provisional dental restorations. *Dental Materials* 37(6):e360-e374, 2021.

Aati S, Shrestha B, Fawzy A: Cytotoxicity and antimicrobial efficiency of ZrO_2 nanoparticles reinforced 3D printed resins. *Dental Materials* 38(8):1432-1442, 2022.

Abduo J, Lyons K, Bennamoun M: Trends in computer-aided manufacturing in prosthodontics: a review of the available streams. *International Journal of Dentistry* 2014, 2014.

Acosta Ortiz R, Savage Gomez AG, Berlanga Duarte ML, Garcia Valdez AE: The effect of a dithiol spiroorthocarbonate on mechanical properties and shrinkage of a dental resin. *Designed Monomers and Polymers* 18(1):73-78, 2015.

Albuquerque PPAC, Moreira ADL, Moraes RR, Cavalcante LM, Schneider LFJ: Color stability, conversion, water sorption and solubility of dental composites formulated with different photoinitiator systems. *Journal of Dentistry* 41:e67-e72, 2013.

Alhavaz A, Rezaei Dastjerdi M, Ghasemi A, Ghasemi A, Alizadeh Sahraei A: Effect of untreated zirconium oxide nanofiller on the flexural strength and surface hardness of autopolymerized interim fixed restoration resins. *Journal of Esthetic and Restorative Dentistry* 29(4):264-269, 2017.

Ali Sabri B, Satgunam M, Abreeza N, N. Abed A: A review on enhancements of PMMA denture base material with different nano-fillers. *Cogent Engineering* 8(1):1875968, 2021.

Alshamrani A, Alhotan A, Kelly E, Ellakwa A: Mechanical and biocompatibility properties of 3D-printed dental resin reinforced with glass silica and zirconia nanoparticles: in vitro study. *Polymers* 15(11):2523, 2023.

Aydınoğlu A, Yoruç ABH: Effects of silane-modified fillers on properties of dental composite resin. *Materials Science and Engineering: C* 79:382-389, 2017.

Bannunah AM: Biomedical Applications of Zirconia-Based Nanomaterials: Challenges and Future Perspectives. *Molecules* 28(14):5428, 2023.

Beatty M, Swartz M, Moore B, Phillips R, Roberts T: Effect of microfiller fraction and silane treatment on resin composite properties. *Journal of Biomedical Materials Research: An Official Journal of The Society for Biomaterials, The Japanese Society for Biomaterials, and the Australian Society for Biomaterials* 40(1):12-23, 1998.

Calais J, Soderholm K-J: Influence of filler type and water exposure on flexural strength of experimental composite resins. *Journal of Dental Research* 67(5):836-840, 1988.

Chang M-C, Lin L-D, Wu M-T, Chan C-P, Chang H-H, Lee M-S, Sun T-Y, Jeng P-Y, Yeung S-Y, Lin H-J: Effects of camphorquinone on cytotoxicity, cell cycle regulation and prostaglandin E_2 production of dental pulp cells: role of ROS, ATM/Chk2, MEK/ERK and hemeoxygenase-1. *PLoS One* 10(12):e0143663, 2015.

Chen Y, Lu Z, Qian M, Zhang H, Chen C, Xie H, Tay FR: Chemical affinity of 10-methacryloyloxydecyl dihydrogen phosphate to dental zirconia: Effects of molecular structure and solvents. *Dental Materials* 33(12):e415-e427, 2017a.

Chen Y, Lu Z, Qian M, Zhang H, Xie H, Chen C: Effect of 10-methacryloxydecyl dihydrogen phosphate concentration on chemical coupling of methacrylate resin to yttria-stabilized zirconia. *The Journal of Adhesive Dentistry* 19(4):349-355, 2017b.

Cramer N, Stansbury J, Bowman C: Recent advances and developments in composite dental restorative materials. *Journal of Dental Research* 90(4):402-416, 2011.

Dawood A, Marti BM, Sauret-Jackson V, Darwood A: 3D printing in dentistry. *British Dental Journal* 219(11):521-529, 2015.

de Castro DT, Valente ML, Agnelli JAM, da Silva CHL, Watanabe E, Siqueira RL, Alves OL, Holtz RD, Dos Reis AC: In vitro study of the antibacterial properties and impact strength of dental acrylic resins modified with a nanomaterial. *The Journal of Prosthetic Dentistry* 115(2):238-246, 2016.

Dejak B, Młotkowski A, Romanowicz M: Finite element analysis of stresses in molars during clenching and mastication. *The Journal of Prosthetic Dentistry* 90(6):591-597, 2003.

Della Bona A, Cantelli V, Britto VT, Collares KF, Stansbury JW: 3D printing restorative materials using a stereolithographic technique: a systematic review. *Dental Materials*, 2021.

Ergun G, Sahin Z, Ataol AS: The effects of adding various ratios of zirconium oxide nanoparticles to poly(methyl methacrylate) on physical and mechanical properties. *Journal of Oral Science* 60(2):304-315, 2018.

Eshmawi YT, Al-Zain AO, Eckert GJ, Platt JA: Variation in composite degree of conversion and microflexural strength for different curing lights and surface locations. *The Journal of the American Dental Association* 149(10):893-902, 2018.

Ferracane J: Elution of leachable components from composites. *Journal of Oral Rehabilitation* 21(4):441-452, 1994.

Ferracane JL: Resin composite—State of the art. *Dental Materials* 27(1):29-38, 2011.

Fujioka-Kobayashi M, Miron RJ, Lussi A, Gruber R, Ilie N, Price RB, Schmalz G: Effect of the degree of conversion of resin-based composites on cytotoxicity, cell attachment, and gene expression. *Dental Materials* 35(8):1173-1193, 2019.

Gad MM, Al-Thobity AM, Rahoma A, Abualsaud R, Al-Harbi FA, Akhtar S: Reinforcement of PMMA Denture Base Material with a Mixture of ZrO_2 Nanoparticles and Glass Fibers. *International Journal of Dentistry* 2019:2489393, 2019.

Gomes AL, Castillo-Oyagüe R, Lynch CD, Montero J, Albaladejo A: Influence of sandblasting granulometry and resin cement composition on microtensile bond strength to zirconia ceramic for dental prosthetic frameworks. *Journal of Dentistry* 41(1):31-41, 2013.

Gonçalves F, Kawano Y, Pfeifer C, Stansbury JW, Braga RR: Influence of BisGMA, TEGDMA, and BisEMA contents on viscosity, conversion, and flexural strength of experimental resins and composites. *European Journal of Oral Sciences* 117(4):442-446, 2009.

Gurushantha K, Anantharaju KS, Nagabhushana H, Sharma SC, Vidya YS, Shivakumara C, Nagaswarupa HP, Prashantha SC, Anilkumar MR: Facile green fabrication of iron-doped cubic ZrO_2 nanoparticles by Phyllanthus acidus: Structural, photocatalytic and photoluminescent properties. *Journal of Molecular Catalysis A: Chemical* 397:36-47, 2015.

Habib E, Wang R, Wang Y, Zhu M, Zhu X: Inorganic fillers for dental resin composites: present and future. *ACS Biomaterials Science & Engineering* 2(1):1-11, 2016.

Inokoshi M, De Munck J, Minakuchi S, Van Meerbeek B: Meta-analysis of bonding effectiveness to zirconia ceramics. *Journal of Dental Research* 93(4):329-334, 2014.

ISO 10993-5:2009. Biological evaluation of medical devices - Part 5: Tests for in vitro cytotoxicity. *International Organization for Standardization, Geneva,* 2009.

ISO 10993-12:2012. Biological evaluation of medical devices - Part 12: Sample preparation and reference materials. *International Organization for Standardization, Geneva,* 2012.

ISO 4049:2019. Dentistry - Polymer-based restorative materials. *International Organization for Standardization, Geneva,* 2019.

Keiteb AS, Saion E, Zakaria A, Soltani N: Structural and Optical Properties of Zirconia Nanoparticles by Thermal Treatment Synthesis. *Journal of Nanomaterials* 2016:1913609, 2016.

Kessler A, Hickel R, Reymus M: 3D Printing in Dentistry—State of the Art. *Operative Dentistry* 45(1):30-40, 2020.

Kim G-T, Go H-B, Yu J-H, Yang S-Y, Kim K-M, Choi S-H, Kwon J-S: Cytotoxicity, Colour Stability and Dimensional Accuracy of 3D Printing Resin with Three Different Photoinitiators. *Polymers* 14(5):979, 2022.

Lin C-H, Lin Y-M, Lai Y-L, Lee S-Y: Mechanical properties, accuracy, and cytotoxicity of UV-polymerized 3D printing resins composed of Bis-EMA, UDMA, and TEGDMA. *The Journal of Prosthetic Dentistry* 123(2):349-354, 2020.

Liu M, Wang Y, Zhang H, Liu X, Wei Q, Li M, Liu Z, Bao C, Zhang K: Effects of dispersant concentration on the properties of hydroxyapatite slurry and scaffold fabricated by digital light processing. *Journal of Manufacturing Processes* 109:460-470, 2024.

Maji P, Choudhary RB, Majhi M: Structural, optical and dielectric properties of ZrO_2 reinforced polymeric nanocomposite films of polymethylmethacrylate (PMMA). *Optik* 127(11):4848-4853, 2016.

Mizobuchi S, Ohtani M, Kobiro K: Contribution of micropores in porous zirconia spheres to high optical transparency of dental resin composites. *Dental Materials Journal* 43(1):119-125, 2024.

Moon W, Kim S, Lim B-S, Park Y-S, Kim RJ-Y, Chung SH: Dimensional Accuracy Evaluation of Temporary Dental Restorations with Different 3D Printing Systems. *Materials* 14(6):1487, 2021.

Mubarak S, Dhamodharan D, B. Kale M, Divakaran N, Senthil T, P S, Wu L, Wang J: A novel approach to enhance mechanical and thermal properties of SLA 3D printed structure by incorporation of metal–metal oxide nanoparticles. *Nanomaterials* 10(2):217, 2020.

Nagaoka N, Yoshihara K, Feitosa VP, Tamada Y, Irie M, Yoshida Y, Van Meerbeek B, Hayakawa S: Chemical interaction mechanism of 10-MDP with zirconia. *Scientific Reports* 7(1):1-7, 2017.

Palmero P, Fornabaio M, Montanaro L, Reveron H, Esnouf C, Chevalier J: Towards long lasting zirconia-based composites for dental implants. Part I: Innovative synthesis, microstructural characterization and in vitro stability. *Biomaterials* 50:38-46, 2015.

Park M-E, Shin S-Y: Three-dimensional comparative study on the accuracy and reproducibility of dental casts fabricated by 3D printers. *The Journal of Prosthetic Dentistry* 119(5):861. e861-861. e867, 2018.

Pilo R, Kaitsas V, Zinelis S, Eliades G: Interaction of zirconia primers with yttria-stabilized zirconia surfaces. *Dental Materials* 32(3):353-362, 2016.

Punia U, Kaushik A, Garg RK, Chhabra D, Sharma A: 3D printable biomaterials for dental restoration: A systematic review. *Materials Today: Proceedings* 63:566-572, 2022.

Randolph LD, Palin WM, Leloup G, Leprince JG: Filler characteristics of modern dental resin composites and their influence on physico-mechanical properties. *Dental Materials* 32(12):1586-1599, 2016.

Reymus M, Fabritius R, Keßler A, Hickel R, Edelhoff D, Stawarczyk B: Fracture load of 3D-printed fixed dental prostheses compared with milled and conventionally fabricated ones: the impact of resin material, build direction, post-curing, and artificial aging—an in vitro study. *Clinical Oral Investigations* 24:701-710, 2020.

Ribas-Massonis A, Cicujano M, Duran J, Besalú E, Poater A: Free-Radical Photopolymerization for Curing Products for Refinish Coatings Market. *Polymers* 14(14):2856, 2022.

Rodríguez HA, Kriven WM, Casanova H: Development of mechanical properties in dental resin composite: Effect of filler size and filler aggregation state. *Materials Science and Engineering: C* 101:274-282, 2019.

Seo J-Y, Oh D, Kim D-J, Kim K-M, Kwon J-S: Enhanced mechanical properties of ZrO2-Al2O3 dental ceramic composites by altering Al_2O_3 form. *Dental Materials* 36(4):e117-e125, 2020.

Shah PK, Stansbury JW: Role of filler and functional group conversion in the evolution of properties in polymeric dental restoratives. *Dental Materials* 30(5):586-593, 2014.

Stansbury JW, Idacavage MJ: 3D printing with polymers: Challenges among expanding options and opportunities. *Dental Materials* 32(1):54-64, 2016.

Teshima I: Degradation of 10-methacryloyloxydecyl dihydrogen phosphate. *Journal of Dental Research* 89(11):1281-1286, 2010.

Thompson JY, Stoner BR, Piascik JR, Smith R: Adhesion/cementation to zirconia and other non-silicate ceramics: Where are we now? *Dental Materials* 27(1):71-82, 2011.

Tian F-c, Wang X-y, Huang Q, Niu L-n, Mitchell J, Zhang Z-y, Prananik C, Zhang L, Chen J-h, Breshi L, Pashley DH, Tay FR: Effect of nanolayering of calcium salts of phosphoric acid ester monomers on the durability of resin-dentin bonds. *Acta Biomaterialia* 38:190-200, 2016.

Toledano M, Osorio R, Osorio E, Fuentes V, Prati C, Garcıa-Godoy F: Sorption and solubility of resin-based restorative dental materials. *Journal of Dentistry* 31(1):43-50, 2003.

Tuna SH, Keyf F, Gumus HO, Uzun C: The evaluation of water sorption/solubility on various acrylic resins. *European Journal of Dentistry* 2:191, 2008.

Tzanakakis E-GC, Tzoutzas IG, Koidis PT: Is there a potential for durable adhesion to zirconia restorations? A systematic review. *The Journal of Prosthetic Dentistry* 115(1):9-19, 2016.

Upson SJ, Benning MJ, Fulton DA, Corbett IP, Dalgarno KW, German MJ: Bond Strength and Adhesion Mechanisms of Novel Bone Adhesives. *Bioengineering* 10(1):78, 2023.

Van Noort R: The future of dental devices is digital. *Dental Materials* 28(1):3-12, 2012.

Vitale A, Cabral JT: Frontal conversion and uniformity in 3D printing by photopolymerisation. *Materials* 9(9):760, 2016.

Wang Y, Zhu M, Zhu XX: Functional fillers for dental resin composites. *Acta Biomaterialia* 122:50-65, 2021.

Wille S, Hölken I, Haidarschin G, Adelung R, Kern M: Biaxial flexural strength of new Bis-GMA/TEGDMA based composites with different fillers for dental applications. *Dental Materials* 32(9):1073-1078, 2016.

Wu X, Dai S, Chen Y, He F, Xie H, Chen C: Reinforcement of dental resin composite via zirconium hydroxide coating and phosphate ester monomer conditioning of nano-zirconia fillers. *Journal of the Mechanical Behavior of Biomedical Materials* 94:32-41, 2019.

Xie H, Li Q, Zhang F, Lu Y, Tay FR, Qian M, Chen C: Comparison of resin bonding improvements to zirconia between one-bottle universal adhesives and tribochemical silica coating, which is better? *Dental Materials* 32(3):403-411, 2016.

Xie H, Tay FR, Zhang F, Lu Y, Shen S, Chen C: Coupling of 10-methacryloyloxydecyldihydrogenphosphate to tetragonal zirconia: Effect of pH reaction conditions on coordinate bonding. *Dental Materials* 31(10):e218-e225, 2015.

Yang J, Shen J, Wu X, He F, Xie H, Chen C: Effects of nano-zirconia fillers conditioned with phosphate ester monomers on the conversion and mechanical properties of Bis-GMA- and UDMA-based resin composites. *Journal of Dentistry* 94:103306, 2020.

Ye S, Chuang S-F, Hou S-S, Lin J-C, Kang L-L, Chen Y-C: Interaction of silane with 10-MDP on affecting surface chemistry and resin bonding of zirconia. *Dental Materials* 38(4):715-724, 2022.

Yoshida K, Tsuo Y, Atsuta M: Bonding of dual-cured resin cement to zirconia ceramic using phosphate acid ester monomer and zirconate coupler. *Journal of Biomedical Materials Research Part B: Applied Biomaterials* 77(1):28-33, 2006.

Zidan S, Silikas N, Al-Nasrawi S, Haider J, Alshabib A, Alshame A, Yates J: Chemical Characterisation of Silanised Zirconia Nanoparticles and Their Effects on the Properties of PMMA-Zirconia Nanocomposites. *Materials* 14(12):3212, 2021.

ABSTRACT (IN KOREAN)

10-MDP로 표면 처리된 지르코니아 필러의 처리 시간에 따른 3D 프린팅 레진의 특성

<지도교수 권 재 성>

연세대학교 대학원 응용생명과학과

김 기 태

3D 프린팅 시스템은 제작 과정을 간소화하고 제작 시간을 단축하며 개인 맞춤형 제작이 가능하여 치과 분야에서 널리 활용되고 있다. 고정성 치과 보철물 제작에는 3D 프린팅 레진의 기계적 특성, 물리적 특성, 중합률, 정확도 및 생체 적합성이 중요하다. 특히, 치과 보철물은 구강 내에서 교합력을 견딜 수 있어야 하기 때문에 기계적 특성을 향상시키는 연구가 필요하다. 3D 프린팅 레진에 첨가된 지르코니아 필러는 우수한 기계적 성질, 생체적합성, 뛰어난 내마모성 등의 다양한 장점을 가지고 있다. 그러나 지르코니아 필러는 실란 커플링제와 화학적 친화력이 부족하다. 이러한 한계를 극복하기 위해 10-Methacryloyloxydecyl dihydrogen phosphate (10-MDP)를 지르코니아 필러의 표면 개질제로 사용했다. 10-MDP 분자의 한쪽 끝에 인산기를 가지고 있어 지르코니아와 화학적 결합을 형성할 수 있고,

다른 쪽 끝에는 메틸 메타크릴레이트기가 있어 레진 매트릭스와 중합할 수 있다. 따라서 10-MDP 로 지르코니아 필러를 표면 처리하면 지르코니아 표면이 개질될 것으로 기대된다. 본 연구의 목적은 10-MDP 를 표면 개질제로 다양한 노출시간을 설정하여 최적화된 표면처리 지르코니아 필러를 제작하고, 표면처리된 필러를 3D 프린팅 레진에 첨가하여 기계적 특성을 향상시키는 것이다.

지르코니아 필러는 10-MDP solution 을 이용하여 표면처리 하였다. 대조군은 상업용 3D 프린팅 레진을 사용하였고, 실험군은 처리되지 않은 지르코니아 필러가 추가된 0D 그룹과 각각 1 일, 7 일, 14 일 동안 표면 처리된 지르코니아 필러를 포함하는 1D, 7D, 14D 그룹으로 설정하였다. 필러의 표면처리를 확인하기 위해 투과 전자 현미경(Transmission Electron Microscopy, TEM), 열중량 분석기(Thermogravimetric Analyzer, TGA), X 선 광전자 분광기(X-ray Photoelectron Spectroscope, XPS) 분석을 실시하였다. 표면처리된 지르코니아 필러 5 wt.%를 상업용 3D 프린팅 레진과 혼합하였다. 시편은 CAD 프로그램을 사용하여 디자인하고 DLP 3D 프린터로 2 출력하였다. 이후 3D 프린팅된 시편에 대해 후처리 공정을 수행하였다. 실험에서는 기계적 특성, 물 흡수도 및 용해도, 중합률, 치수 정확도 및 세포 독성을 측정하였다.

표면처리된 지르코니아 필러는 TEM 이미지에서 유기화합물이 부착되어 있는 것으로 관찰되었다. TGA 결과에서는 100 °C – 450 °C 의 온도 범위에서 중량 감소를 보여주었다. XPS 결과에서는 Zr-O-P 결합이 관찰되었다. TEM, TGA, XPS 분석 결과에 따르면 10-MDP 에 의해 지르코니아 필러의 표면이 성공적으로 개질된 것으로 나타났다. 보관조건과 관계없이 굴곡강도 및 굴곡계수는 0D 그룹에서 일관되게 유의하게 낮았으며, 7D 및 14D 그룹이

다른 그룹에 비해 유의하게 높은 결과를 나타냈다($p < 0.05$). 미세경도는 대조군에서 유의하게 낮은 결과를 보인 반면, 14D 그룹에서는 유의하게 높은 결과를 보였다($p < 0.05$). 물 흡수도에서 7D 와 14D 그룹은 대조군에 비해 유의하게 낮은 값을 보였다. 그러나 용해도 시험에서는 1D, 7D, 14D 그룹이 대조군에 비해 유의하게 높은 값을 나타냈다($p < 0.05$). 치수 정확도의 XY 축 결과는 대조군을 제외한 모든 그룹이 참 값에 더 가까웠다($p < 0.05$). 중합률과 세포 독성은 모든 그룹에서 유의한 차이를 보이지 않았다($p > 0.05$).

결론적으로, 10-MDP 를 이용한 지르코니아 필러의 표면처리가 가능함을 입증하였고, 표면처리된 지르코니아를 첨가하면 3D 프린팅 레진의 특성에 영향을 미치는 것으로 나타났다. 또한, 최적의 표면처리 노출시간은 7 일로 판단되었다. 3D 프린팅 레진에 첨가한 10-MDP 로 표면 처리된 지르코니아 필러는 세포독성이 없었으며, 치수 정확도에 부정적 영향 없이 기계적 특성을 향상시킬 수 있는 가능성을 보여주었다. 따라서 10-MDP 로 표면 처리된 지르코니아 필러는 치과용 3D 프린팅 레진의 필러로 충분히 활용될 수 있다.

핵심되는 말: 표면 처리, 10-MDP, 지르코니아 필러, 3D 프린팅 레진, 화학적 결합